HHS Public Access

Author manuscript

Chem Soc Rev. Author manuscript; available in PMC 2018 May 22.

Published in final edited form as:

Chem Soc Rev. 2017 May 22; 46(10): 2824–2843. doi:10.1039/c6cs00675b.

Recent Advances in High-Performance fluorescent and bioluminescent RNA Imaging Probes

Yuqiong Xia[a], **Ruili Zhang**[a], **Zhongliang Wang**[a], **Jie Tian**[a,b], and **Xiaoyuan Chen**[c]

[a]Engineering Research Center of Molecular-imaging and Neuro-imaging of ministry of education, School of Life Science and Technology, Xidian University, Xi'an, Shaanxi, 710126, China

[b]Institute of Automation, Chinese Academy of Sciences, Beijing, 100190, China

[c]Laboratory of Molecular Imaging and Nanomedicine (LOMIN), National Institute of Biomedical Imaging and Bioengineering (NIBIB), National Institutes of Health (NIH), Bethesda, MD, 20892, USA

Abstract

RNA plays an important role in life processes. Imaging of messenger RNAs (mRNAs) and micro-RNAs (miRNAs) not only allows us to learn the formation and transcription of mRNAs and the biogenesis of miRNAs involved in various life processes, but also helps in detecting cancer. High-performance RNA imaging probes greatly expand our view of life processes and enhance the cancer detection accuracy. In this review, we summarize the state-of-the-art high-performance RNA imaging probes, including exogenous probes that can image RNA sequences with special modification and endogeneous probes that can directly image endogenous RNAs without special treatment. For each probe, we review its structure and imaging principle in detail. Finally, we summarize the application of mRNA and miRNA imaging probes in studying life processes as well as in detecting cancer. By correlating the structures and principles of various probes with their practical uses, we compare different RNA imaging probes and offer guidance for better utilization of the current imaging probes and the future design of higher-performance RNA imaging probes.

Graphical abstract

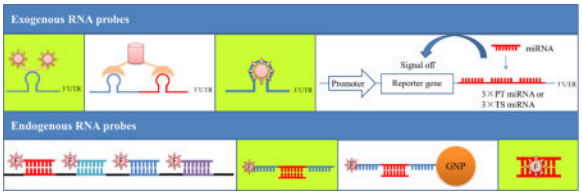

1 Introduction

RNA plays an important role in gene expression and regulation. For gene expression, mRNAs are the templates, while tRNAs and rRNAs are the transporters of amino acids and the catalysts, respectively. For gene regulation, siRNA (small interfering RNA), miRNA

Correspondence to: Zhongliang Wang; Jie Tian; Xiaoyuan Chen.

(microRNA) and shRNA (small hairpin RNA) can modulate gene expression in different ways. Learning gene expression and regulation not only increases the understanding of various life processes, but also helps in disease diagnosis and therapy[1–3].

Visualization of gene expression and regulation can be implemented by imaging various RNAs[4–9], mostly mRNAs[4] and miRNAs[5, 10, 11]. The mRNAs play a central role in gene expression and regulation, and therefore learning the transcription[6], localization[7], transport[8] and translation[9] offers a lot of information on gene expression. The miRNAs are endogenous regulating RNAs that control the gene expression of mRNAs, and therefore the imaging of miRNAs tells a lot about the gene regulation of the corresponding mRNAs[5, 10, 11].

In nature, RNAs themselves do not give out specific signals to enable imaging. Instead, imaging probes are specially designed to allow researchers to “see” the RNAs. Generally, most imaging probes have two necessary parts: the RNA-binding part and the imaging part. The RNA-binding part is mostly composed of RNA or DNA sequences that can bind to target RNAs or be inserted into target RNA sequences. On the other hand, the imaging part is much less constricted. All the imaging probes, such as fluorescence dyes, fluorescence proteins, bioluminescence dyes and fluorescence NPs, can be used as imaging parts only if they are stably conjugated to the RNA-binging part. In some cases, to improve the signal to noise ratio, a third part that can enhance the entire imaging signal or reduce the background signal is added.

RNA imaging probes can be divided into two types: probes imaging exogenous RNAs and probes imaging endogenous RNAs. They are quite different in structure and principle and are explained separately in this review. In the former type of RNA imaging probes, the target RNAs are not natural endogenous RNAs, but are RNAs with the external insertion of certain protein binding sequences, dye-binding sequences or dye-expressing sequences. The imaging probes then specifically interact with the inserted RNA sequence (except for the dye-expressing sequence), illuminating target RNAs. Currently, probes imaging exogenous RNAs include the RBP-FP (RNA binding protein-fluorescent protein) system, bimolecular fluorescence complementation (BiFC), RNA aptamer/fluorophore system and reporter gene system. However, in the latter type of RNA imaging probes, the endogenous RNAs are natural endogenous RNAs and do not need extra pre-treatment before imaging. The imaging probes generally bind to the target RNAs through base-pair complementation. This type of probe includes fluorescence *in situ* hybridization (FISH) probes, molecular beacons (MBs) and nano molecular beacons (Nano-MBs) and quencher-free probes. Fig. 1 summarizes the two types of general high-performance RNA imaging probes and their brief applications, as discussed in this review.

It is worth noting that this review mainly focuses on fluorescent and bioluminsescent RNA imaging probes, but there are several promising RNA nanoprobes with other optical methods such as surface-enhanced Raman scattering (SERS)[12–15] and dark field[16–18] methods. SERS-based RNA imaging probes have two distinct types: label-free SERS probes[13–15] and nanotag-containing SERS probes[17, 18]. The former utilizes the distinct SERS signals of four miRNA bases upon adsorption to SERS substrates such as gold and silver. The nanotags in the latter type of Raman probe are generally Raman-active compounds and recognition

nucleotide sequences, which image target RNAs through base-pairing and are structurally similar to the Nano-MBs in this study. Dark-field based RNA imaging probes[16] are generally GNPs modified with recognition nucleotide sequences, which have plasmon coupling and change scattering signals in the presence of target RNAs. Both SERS-based and dark-field based RNA imaging probes are highly specific, highly sensitive and multiplexed and their applications mainly focus on the detection of miRNA tumour markers. Moreover, DNA-modified GNP based bio-barcode assay, which used a conventional gel electrophoresis platform and potassium cyanide chemistry, can also detect miRNA tumour markers with high specificity and sensitivity[19]. In contrast, fluorescent and bioluminescent RNA imaging probes have similar advantages, but have wider applications due to their more versatile structures. In this review, we first introduce the probes imaging exogenous RNAs, followed by probes imaging endogenous RNAs. After that, we analyze the application of the RNA imaging techniques in tracking RNA processes and cancer diagnosis. Finally, we briefly summarize this review and give some suggestions on the design of RNA imaging probe in different cases. Furthermore, we provide an outlook for the development of RNA imaging *in vivo* with even more sensitive imaging probes and advanced imaging technologies. There are also some other related excellent reviews, including RNA detection on a chip[20], live-cell RNA imaging[21–27], probes for biomolecular detection[28–31] and miRNA imaging.[32, 33]

2 Probes imaging exogenous RNAs

Exogenous RNAs are RNAs with the external insertion of a certain protein-binding sequence, dye-binding sequence or dye-expressing sequence. Currently, probes imaging exogenous RNAs can be classified into four types: RBP-FP system, bimolecular fluorescence complementation (BiFC) system, RNA aptamer/fluorophore system and reporter gene system. For the RBP-FP system, the imaging probes specifically interact with the inserted protein-binding sequence and then illuminate target RNAs. For BiFC, the imaging probes are divided into two non-fluorescent parts and specifically interact with two different inserted protein-binding sequences in the same target RNAs. The BiFC probe will illuminate target RNAs only when the two parts of the imaging probes reunite correctly and it has much lower background than the RBP-FP system. For the RNA aptamer/fluorophore system, the imaging fluorophore interacts directly with the inserted RNA aptamer (dye-binding sequence) and illuminates the target RNA. This system images much faster than the RBP-FP system and BiFC system and can therefore be used in real-time imaging. For the reporter gene system, the inserted dye-expressing sequence can express fluorophores (such as GFP) or luciferase. After insertion into 3′UTR of reporter genes, the regulating miRNA can be indirectly imaged. Since all these probes must work in cooperation with their corresponding RNAs with proper pre-treatment, they are classified as probes imaging exogenous RNAs.

2.1 RNA binding protein-fluorescent protein system (RBP-FP system)

As shown in Fig. 2a[34], the RBP is an MS2 coat protein (MCP) that can specifically bind to MBS (MS2 binding sequence, an RNA sequence) and the FP is GFP. To image target mRNA, the mRNA was pre-treated to contain six units of MBS in the 3′-UTR (untranslated

region), and then the MCP-GFP fusion protein was added into the cells containing pre-treated mRNA. The MCP-GFP fusion protein then binds to the target mRNA and illuminates the target mRNAs. Fig. 2a shows the binding of MCP-GFP fusion protein to six units of MBS in the 3′-UTR of target mRNAs through the interaction between MCP and MBS. With this system, the localization and transport of *ASH1* mRNA particles in living yeast was tracked[34].

The increase of binding fluorophores can further enhance the signal in the RBP-FP system. Singer and his colleagues inserted 24 repeats of MBS in the 3′-UTR of one single mRNA molecule so that one mRNA molecule could bind 24 molecules of MCP-YFP[35]. After combing with FISH probes, they realized the detection and localization of single *β-actin* mRNA molecules in various tissues of a mouse[35]. Furthermore, Park *et al.*[36] used the MS2-GFP system to develop a transgenic mouse model where all *β-actin* mRNA (containing MBS in the 3′-UTR) were fluorescently labelled.

MCP-GFP and MCP-YFP combinations, as well as other RBP-FP combinations can be used to image RNAs. Horcine *et al.*[39] realized the dual colour imaging of two MDN1 alleles by applying two RBP-FP pairs. Specifically, they applied two RBP-FPs (green PCP-2yEGFP and red MCP-mCherry) to image two alleles: MDN1-24PP7 (MDN1 with insertion of 24 PP7 binding sequences) and MDN1-24MS2 (MDN1 with insertion of 24 MS2 binding sequences)[39]. Furthermore, a more versatile RBP-FP system was developed by combining small molecule fluorophores with fusion proteins of MS2 and dihydrofolate reductase (MS2-eDHFR) (Fig. 2b) or the SNAP tag (MS2-SNAP). In this system, MS2-eDHFR or MS2-SNAP first binds to target RNA sequences with the insertion of MBS and the RNA remains non-fluorescent. Then, related small molecule fluorophores are added to image the RNA, since the MS2-eDHFR and MS2-SNAP can interact with a wide range of small molecule fluorophores[37]. Since the MS2-eDHFR or MS2-SNAP based system can accommodate a wide range of small molecule fluorophores, red fluorophores can be easily added into this system to reduce cell autofluorescence, which generally has emission wavelengths shorter than 600 nm. The RBP-FP system and its modification systems can image mRNA with high resolution and even track single mRNA movement, and are therefore very suitable for imaging the mRNAs of housekeeping genes whose 3′-UTR is well known and conveniently edited. However, the main disadvantage of this system is that there is always background fluorescence. The reason is that excess RBP-FPs are usually added to the cells or tissues to increase binding efficiency to reporter mRNAs. The unbound RBP-FPs are also fluorescent and therefore contribute to the background. In some cases, background signals can be eliminated by special mathematical methods. For example, the signals of non-mRNA-binding fluorescent proteins can be distinguished from those that are mRNA-binding, according to different diffusion coefficients[40].

2.2 Bimolecular fluorescence complementation system

To reduce the background signal from the RBP-FP system, bimolecular fluorescence complementation (BiFC)[41] was incorporated into RNA imaging[42–44]. In BiFC, FPs are split into two complementary non-fluorescent parts: N-terminal FPs (N-FPs) and C-terminal FPs

(C-FPs). Since neither N-FPs nor C-FPs is fluorescent, the background from free protein becomes negligible.

As shown in Fig. 2c, the BiFC system uses two different RBPs conjugated to two halves of split FPs, namely, RBP1-N-FP and RBP2-C-FP. In the MCP-PCP based BiFC system[45], the two RBPs are MCP and PCP (PP7 bacteriophage coat protein). To image target RNAs, the RNAs are pre-treated with the insertion of MBS and PBS (PP7 binding sequence). First, the N-FP-MCPs and C-FP-PCPs bind to MBS and PBS in the target RNAs, respectively. Next, the bound N-FP and C-FP will be in close proximity and spontaneously fuse to form complete fluorescent FPs[45], imaging the target RNAs.

There is another type of BiFC system in which the interaction between RBP and RNA is based on the aptamer protein interaction, named the aptamer-protein based BiFC system (Fig. 2d). Valencia-Burton *et al.* fused two fragments of eukaryotic initiation factor 4A (eIF4A) to two halves of the split EGFP. The fusion proteins were then bound to target RNA with the eIF4A interactive aptamer sequence inserted in the 3′-UTR of the gene. Binding two fragments of eIF4A to the aptamers brings the EGFR fragments into close proximity to reconstitute a functional FP[38]. As an alternative to the eIF4A based BiFC system, a small viral peptide based BiFC system, was developed. Yiu *et al.* fused HTLV-Rex peptide and lN peptide to two halves of EGFP and successfully imaged target RNA sequences with HTLV-Rex aptamer and lN aptamer in bacteria cells[46].

The abovementioned three types of BiFC system (MCP-PCP based, PUMHD based and aptamer-protein based BiFC system) all apply fusion proteins of RBPs and split FPs and have similar imaging principles, and therefore have lower background compared to RBP-FP systems. However, the BiFC system still has some limitations[45]: (1) it has a diffusive background since free N-FPs and C-FPs at high concentration fuse spontaneously to form FPs in the absence of reporter RNAs; (2) it takes time for N-FP and C-FP to fuse together, and therefore this method is only suitable for the visualization of long-lived RNAs; (3) the fusion of N-FP and C-FP is irreversible and therefore the method is not suitable for visualizing real-time transcription.

2.3 RNA aptamer/fluorophore system

Fig. 3a shows the structure of a RNA aptamer/fluorophore system. The RNA aptamer is pre-inserted in the 3′-UTR of target RNAs and the fluorescence of the fluorophore significantly increases in the presence of target RNA, compared to that in the absence of target RNA. RNA aptamer/fluorophore systems utilize the aptamer-fluorophore interaction, instead of the RNA-RBP interaction in the RBP-FP systems or BiFC systems. The binding between the aptamer and small molecule fluorophore is fast, and therefore this system enables real-time imaging. In this system, RNA aptamers are screened so that they can greatly enhance the fluorescence of fluorophores. The most studied fluorophore is difluoro-4-hydroxybenzylidene imidazolinone (DFHBI) (Fig. 4b), which is a commercial dye mimicking the structure of eGFP.

Spinach aptamer, selected by the SELEX method, is a DFHBI-binding aptamer that enhances the fluorescence of DFHBI 2000 times (Fig. 4a)[47]. Therefore, DFHBI can bind to

Spinach aptamer-fused *5S* RNAs and image their live-cell dynamics[47]. Furthermore, a tandem Spinach array shows up to about 17-fold higher fluorescence by accommodating 8–64 repeats of Spinach aptamers in target RNAs[48]. However, the Spinach aptamer-DFHBI system suffers from limited folding efficiency and thermal instability. The Spinach2 aptamer-DFHBI system can partly solve the problems (Fig. 4a)[49] since both Spinach and Spinach2 aptamers bind to DFHBI depending on the G4 quadruplex structure,[50, 51] which relies on temperature and salt concentration. To overcome the salt-dependency of the Spinach and Spinach2-DFHBI systems, researchers developed the Broccoli aptamer-DFHBI system, which shows brighter fluorescence and less magnesium dependency[52]. The reason is that the Broccoli aptamer (Fig. 4a) does not need extra tRNA arms to fold and does not contain the salt-sensitive G4 quadruplex structure. The more advanced selection method, the microfluidic assisted *In Vitro* Compartmentalization (mIVC) procedure, leads to the selection of the iSpinach aptamer, which is able to work at high temperature and in a potassium free environment[53].

In addition to DFHBI, there are other alternative fluorophores for RNA aptamer/fluorophore systems, such as DFHBI-1T, PFP-DFHBI, and TO1 (Thiazole Orange) (Fig. 4b). DFHBI-1T exhibits lower background fluorescence than DFHBI when incubated with cells[57]. Spinach2-DFHBI-1T exhibits increased fluorescence when imaged with GFP filter cubes due to improved excitation of the complex and lower background fluorescence[57]. PFP-DFHBI exhibits 5-fold higher binding affinity to Spinach2 than DFHBI. Therefore, Spinach2-PFP-DFHBI shows 3–4-fold brighter fluorescence and less salt concentration dependency[58]. TO1 can greatly enhance its fluorescence by binding to G4 quadruplexes containing aptamers. RNA Mango aptamer-TO1 (Fig. 4) exhibits 1,100-fold fluorescence, compared to free TO1, and successfully images the binding and release of *6S* RNA *in vitro*[56].

After conjugation to quenchers, the fluorophores with high background fluorescence can also be applied in RNA aptamer/fluorophore systems (Fig. 3b). Fluorophore-quencher conjugates have low background and can image target RNAs containing fluorophore aptamers. In Sunbul's study, the fluorophore sulforhodamine B (SR) was first conjugated to the quencher dinitroaniline (DN) to form SR-DN conjugates. After binding to the SRB-2 aptamer, the quantum yield of SR-DN increased 25-fold[54]. Alternatively, fluorophore-quencher conjugates can also image target RNAs containing quencher aptamers. In Arora's study[55], the quencher DN was conjugated to a wide range of fluorophores, including fluorescein-dinitroaniline (FL-DN), rhodamine green-dinitroaniline (RG-DN), tetramethylrhodaminedinitroaniline (TMR-DN), sulforhodamine-dinitroaniline (SR-DN) and TexasRed-dinitroaniline (TR-DN). These fluorophores span the entire range of the visible spectrum. After combination with the DN-binding aptamers (DNB aptamers), the fluorophore-DNs can be used to image RNAs in a wide spectral range. Furthermore, two fluorophores with FRET effect can image target RNAs containing fluorophore aptamers, in which the acceptor fluorophores are non-fluorescent in the absence of target RNAs. In Shin's study, Cy3 and Cy5 were used in the live-cell imaging of polymerase II transcriptional activity in real time[59] with their aptamers inserted in target polymerase II mRNA.

In all, RNA aptamer/fluorophore systems have three advantages. First, the fluorescence in this system emerges more rapidly than in the RBP-FP system and BiFC system since the fluorescence only needs transcription of the RNA aptamer and the formation of the fluorophore-RNA aptamer complex is much faster than that of RBP-FP binding to the RNA sequence in the RBP-FP system or that of fusion of N-FPs and C-FPs in BiFC; therefore, the RNA aptamer/fluorophore system is suitable for real-time tracking of RNAs. Second, the background of the RNA aptamer/fluorophore system is low, since the fluorophores have low fluorescence in the freestate or quenched state. Third, the system is resistant to photo-bleaching and is also suitable for long-time tracking of RNAs.

2.4 Reporter gene system

Reporter gene systems are specifically applied in miRNA imaging.[32, 60–63] MiRNAs, which are generally 21–25 nt single-stranded RNAs, are sequence specific regulators that can control the regulation of various genes[64, 65]. Therefore, the reporter gene systems mostly focus on the imaging of the function of mature miRNAs,[66–71] although imaging of pri-miRNA (primary miRNA) transcription, pri-miRNA cutting, ds-miRNA (miRNA-miRNA*) and miRNA function that destabilizes mRNA or inhibits target genes are also studied.[60] In this section, we focus on the imaging of single-stranded miRNA function by reporter gene systems.

Fig. 5a shows the typical structure of a reporter gene system. A strong promoter (usually CMV) was inserted into the 5′-end of the reporter gene and three repeats of miRNA target sequences (3×TS_miRNA) or miRNA perfect targets (3×PT_miRNA) were inserted into the 3′-UTR of the reporter gene (CMV/Reporter gene/3×TS_miRNA). Genes of GFP or luciferase (Fluc, Gluc and Rluc) are often used as reporter genes, with the former expressing fluorescent proteins and the latter emitting bioluminescence in the presence of corresponding substrates (coelenterazine for Rluc or Gluc and D-luciferin for Fluc)[63]. In the presence of target miRNAs, the miRNAs will bind to the 3×TS_miRNA and inhibit the gene expression of reporter genes, leading to a reduction in fluorescence signal or bioluminescence signal. Bioluminescent reporter gene systems are more suitable for miRNA imaging *in vivo* than fluorescent reporter gene systems[72] since the reporter gene system is a negative system and the background of the former is much less than that of the latter.

Kim *et al.*[68] applied a CMV/Gluc/3×PT_miR221 reporter gene system and found overexpression of miR221 in papillary thyroid carcinoma (PTC), demonstrating that the reporter gene system can be used to quantify endogenous miRNAs *in vitro* and *in vivo*. Tu *et al.*[69] applied a CMV/Gluc/3×PT_miR22 reporter gene system and observed overexpression of miR22 in cardiac hypertrophy. They further used antagomir-22 to knock down miR-22 and reversed the repressed Gluc activities *in vitro* and *in vivo*. Ko *et al.* applied a CMV/Gluc/3×PT_mi124a reporter gene system[71], illustrating the miR124a-dependent decrease of Gluc reporter activity during neuronal differentiation[70]. Wang *et al.* developed a CMV/Fluc/3×TS_miR21 reporter system to image anti-miR21[67]. Once exogenous anti-miR-21 oligonucleotides carried by GO-PEG-dendrimer enter the cells, they inhibit the functions of miR-21, and therefore block miR-21 from binding to the 3′-UTR of luciferase, activating the luciferase reporter and inducing bioluminescence[67].

The reporter gene systems can also be coupled with other reporter gene systems or other imaging methods to offer more information on miRNA imaging. Lee *et al.*[73] (Fig. 5b) applied a CMV/Gluc/3×PT_miR23a reporter gene system and miR23a promoter/Fluc to monitor expression and posttranscriptional regulation of miR23a, which reveals information on transcription of pri-miR23a, which is very useful in tracking the behaviour of miR23 during differentiation. Wang *et al.*[74] constructed a dual reporter gene system in one vector as ubiquitin/hNIS/Fluc/3×TS_miR16 (Fig. 5c). Using positron emission tomography (PET) imaging through hNIS and bioluminescence imaging through Fluc, the miR16 was quantified and the involvement of miR16 in the chemoresistance of gastric cancer was demonstrated.

The exogenous RNA imaging systems mentioned above have quite distinct structures and principles. Each imaging system works for certain RNA imaging. For RNA imaging by the RBP-FP system, BiFC system and RNA aptamer/fluorophore system, the RNAs need to accommodate corresponding RNA sequences without affecting the properties of RNAs. For short RNAs, like miRNAs, siRNAs, and shRNAs, these systems are not suitable, since the added sequence will significantly change the properties of the RNAs. For long RNAs, such as mRNAs, rRNAs and tRNAs, although extra RNA sequences can be easily inserted into the sequences, it is unknown whether these insertions will lead to malfunction of the RNAs. Therefore, the RBP-FP system, BiFC system and RNA aptamer/fluorophore system are more often used to image well-known mRNAs and rRNAs as well as tRNAs, whose lengths and non-functional sequences are clear. It should be noted that reporter gene imaging systems only work for miRNAs, but not other for RNAs.

3. Probes imaging endogenous RNAs

Unlike probes imaging exogenous RNAs, probes imaging endogenous RNAs do not need to incorporate certain RNA sequences in target RNAs or transcribe reporter genes. They contain recognition sequences and image endogenous RNAs through base-pairing complementation.

In this section, we introduce FISH probes, MBs, nano-MBs and quencher-free probes. FISH probes are generally ssDNAs or ssRNAs tagged with fluorophores and can image target RNAs with high resolution due to the presence of a large amount of probes. FISH probes are often applied to image RNAs in fixed cells. MBs are ssDNAs or ssRNAs with stem-loop structures (or β-hairpin structures), where a fluorophore and a quencher are in the stem part and the recognition sequence lies in the loop area. The MB is not fluorescent at the stem-loop structure, but becomes fluorescent in the presence of target RNAs; therefore, MB probes also have low background signals. MBs cannot enter cells themselves, and therefore for live-cell imaging, a gene carrier is needed to deliver the probes. Furthermore, nano-MBs refer to those MBs in which NPs are incorporated to act as both the quencher and the carrier, and no additional gene carriers are needed to deliver the probes. Nano-MBs also have very low background. Quencher-free probes are ssDNAs or ssRNAs that contain special fluorophores, which are non-fluorescent in ssDNA or ssRNA structure, but become fluorescent in DNA/RNA duplex or dsRNA structure. Typical quencher-free probes include

single dye forced intercalation (FIT) probes and exciton-controlled hybridization-sensitive fluorescent oligonucleotide (ECHO) probes.

3.1 FISH probes

FISH technology was developed in 1980s and was initially used in genome imaging[27, 75]. FISH probes for RNA imaging are a group of ssDNA, ssRNA or hybrid ssRNA/DNA sequences tagged with same fluorophores, with the sequences complementary to different parts of the target RNAs (Fig. 6a).

Since FISH probes are fluorescent in the absence of target RNAs, the background signal would be high if the free FISH probes are not removed. Therefore, FISH probes can only image RNAs in fixed-cells where the cells are under pre-treatment and the free FISH probes can be removed. For general RNA imaging with FISH probes, a typical procedure is as follows (Fig. 6b)[33]: first, there is cell fixation and permeabilization, where tissues or cells are fixed and lipids in the membrane are then removed to increase cell permeability. This step is a must, since FISH probes are negatively charged DNA or RNA sequences and they cannot automatically enter live cells. Cell permeaiblization allows FISH probes to enter cells through the holes on the cell surface. Second, there is hybridization of FISH probes with target RNAs, where FISH probes are added to pre-treated cells and allowed to hybridize with target RNAs. This step (Fig. 6b) is necessary to remove all the unbound FISH probes, except for FRET-based FISH probes[76], whose background signals are low. Third, there is the removal of weakly bound FISH probes, where non-specifically bound FISH probes and free FISH probes are washed away. Finally, there is the detection of target RNAs, where the pre-treated samples are then observed under fluorescence microscope[33].

FISH probes often have high sensitivity because several oligonucleotide probes are located on adjacent sequences on an RNA target such that their collective fluorescence will be emitted as a point source after hybridization. Therefore, they can be used to quantify the copy numbers of target RNAs. Femino *et al.*[77] used 10 FISH probes (61–64 nt, each with 6 Cy3) to hybridize with *β-actin* mRNA and 11 FISH probes (50–61 nt, each with 5 FITC) to label the *β-actin* nascent transcript (Fig. 6a), not only quantifying the copy numbers of the mRNA and the transcript, but also learning the transcription kinetics of *β-actin* mRNA. Similarly, Treck *et al.*[78] used 4–10 FISH probes (50 nt, each with 4–5 fluorophores) and quantified the copy numbers of single-mRNAs in budding yeast cells. However, this method has two caveats: high nonspecific binding to non-target RNAs and complicated synthesis of probes[79].

To reduce nonspecific binding and simplify the synthesis of FISH probes, much shorter probes tagged with the same single fluorophore were used to image single molecular mRNA. It turned out that the improved probes can image single molecular mRNA at high resolution, and the nonspecific binding is negligible[79]. Similarly, three sets of probes, each containing 48 FISH probes (20 nt) labelled with the same fluorophores, were applied to imaging three mRNAs (*ERBB2*(red), *AKT1* (green) and *AKT3* (blue) mRNA) simultaneously. Moreover, they accurately quantified two of the mRNAs (*ERBB2* and *AKT1* mRNA), which were in accordance with the results of the immunoFISH method[80].

Chemical modifications of FISH probes[81] can greatly improve their imaging properties[33]. Fig. 6c shows typical chemical modifications on nucleic acid, where 2′-O-methyl RNA (2′-OMe RNA) and 2′-F RNA have better chemical stability than unmodified RNA; lock nucleic acid (LNA) and peptide nucleic acid (PNA) are modified on the bone structure and also have better chemical stability than common nucleic acid (DNA or RNA). After the incorporation of 2′-F RNA in ssDNA FISH probes, the 2′-F RNA/DNA probes have increased binding and better nuclease resistance than conventional hybrid ssRNA/DNA FISH probes[82]. Similarly, ssLNA (locked nucleic acid)/DNA FISH probes also have faster hybridization and higher efficiency[83], and 2′-O-methyl RNA/LNA FISH probes have higher affinity for target RNA[84].

Employment of a nucleic acid amplification method can substantially increase the signal of FISH probes. Choi *et al.* incorporated the hybridization chain reaction (HCR) method into FISH probes for signal amplification (Fig. 7a)[85]. In detail, the FISH probes include three parts: initiator containing recognition sequence, H1 hairpin with one fluorophore and H2 hairpin with the same fluorophore. To image target RNA, the initiator is first allowed to hybridize with target RNA, and then the H1 strand and H2 strand are sequentially and repeatedly bound to the hybrid duplex. Later, a long amplification polymer containing alternative H1 and H2 strands with multiple fluorophores for one target RNA is formed, leading to signal amplification. Using five sets of such FISH probes with distinguished fluorophores, five target mRNAs were imaged successfully in fixed whole-mount and sectioned zebrafish embryos[85]. Ge *et al.* incorporated the rolling cycle amplification (RCA) method (Fig. 7b) into FISH probes to image miR-222 in SMMC-7721 human hepatoma cells and L02 hepatocyte cells[86]. The components in this RCA method include a circular DNA, dNTP, DNA polymerase and detection probe (ssDNA labelled with fluorophore). For target miRNA imaging, the circular DNA will first bind to target miRNA and then a long tandem duplex with numerous fluorophores will be synthesized through *in situ* RCA, enabling signal magnification for each miRNA molecule. Similarly, Deng *et al.* also successfully imaged let-7a miRNA using RCA amplification[87].

Enzyme-mediated signal amplification can also be employed in FISH probes to increase sensitivity. Tyramide signal amplification (TSA)[10, 88] and enzyme-labelled fluorescence (ELF) signal amplification,[11, 89] two outstanding and complementary amplification methods, are often combined with FISH probes. In TSA, target RNA is first hybridized by a primary-antibody conjugated nucleic acid probe, and then secondary-antibody-conjugated horseradish peroxidase (HRP) is further attached through antigen-antibody interaction. After that, fluorescent dye labelled tyramide is added, whose fluorescence will significantly increase in the presence of the catalyst HRP. In this way, TSA realizes signal amplification of target RNA utilizing the HRP enzyme. Using TSA, LNA FISH probes can image miR-124a in frozen brain tissues[10] more rapidly and efficiently than the same probes without TSA. Similarly, LNA FISH probes with TSA are also shown to image miR-142 in neurons and other cell types with higher sensitivity than LNA FISH probes without TSA[88]. On the other hand, in ELF, target RNA is also first hybridized by primary-antibody-conjugated nucleic acid probe, and then secondary-antibody-conjugated phosphatase is further attached. After that, ELF-97 (enzyme labelled fluorescence) phosphatase substrate[90] is added, which is converted to brightly and stably fluorescent ELF alcohol in the presence

of phosphatase. Using ELF amplification, individual miR-15a and miR-155 were identified as bright and photostable fluorescent spots in single cells[11].

In addition, RNA FISH probes can be easily modified with different fluorophores and combined with mathematical treatments (binary colour combinations and ratio identity codes)[75]. In this way, RNA FISH probes can be used to image thousands of RNA sequences simultaneously. Lubeck *et al.*[91] applied the sequential hybridization of FISH probes and obtained robust and high signal RNA images. During each round of hybridization, FISH probes with single fluorophores are hybridized with target RNAs; then, the FISH probes are digested and in a new round of hybridization, new FISH probes with same sequences but a different single fluorophore are hybridized with the same target RNAs. With the sequential hybridization method, they successfully barcoded 12 genes in single yeast cells with four dyes and two rounds of hybridization. Furthermore, Chen *et al.*[92] developed multiplexed error-robust FISH (MERFISH), a single-molecule imaging method that allows thousands of RNA species to be imaged in single cells using combinatorial FISH labelling with encoding schemes capable of detecting and/or correcting errors.

In summary, FISH probes for RNA imaging have very high sensitivity and can quantify the copy numbers of mRNAs and image low-content miRNAs with signal amplification methods. Multiplexed FISH probes combined with mathematical methods can be used to simultaneously image multiple RNAs. They have standard synthesis procedures and are versatile enough to image different target RNAs. The only limitation is that FISH probes cannot be used in live-cell imaging, and successful imaging of RNAs by FISH probes will need careful pre-treatment of cells.

3.2 Molecular beacons (MBs)

Molecular beacons are the most-studied probes for RNA imaging[93–96]. They have stem-loop DNA structures (or β-hairpin structures, Fig. 8a) with recognition sequences lying in the loop areas. In the stem area, the fluorophore and quencher are in close proximity, leading to non-fluorescent MBs at first. However, once the MBs are exposed to target RNAs, the recognition sequence will form a stable hybrid duplex with target RNAs, and the stem-loop structure will become linear, forcing the quencher to be away from the fluorophore, and therefore restoring the fluorescence of the fluorophore. A modification of MB is the dsDNA probe containing a recognition strand and a quencher strand (Fig. 8b)[97]. The recognition strand carries a FRET donor and its sequence is complementary to that of target RNA. The quencher strand carries a FRET acceptor, quenching the fluorescence of the recognition strand. In the presence of the target RNA, the recognition strand will form a hybrid duplex with the target RNA and release the quencher strand, imaging the target RNA.

Backbone modification of MBs can increase the affinity and specificity, accelerate hybridization kinetics, and reduce fluorescence background. For instance, a chimeric RNA-DNA MB (chMB, Fig. 8c) with RNA loop and DNA stem was shown to have a higher fluorescence signal than typical DNA-MB hybrids and was applied to imaging nucleic acids[98]. LNA-MBs with a part of the nucleic acids substituted with LNAs (Fig. 8d) have better cellular stability and can track RNAs for a longer period of time[99]. Stemless PNA MBs (Fig. 8e) were shown to have lower background than common MBs[100]. The reason lies

in their special fluorescent donors, which are non-fluorescent when bound to ssDNAs, but become fluorescent when embedded in dsDNAs. Since stemless PNA MBs do not contain FRET acceptors with background fluorescence, they have much lower background than common stem-loop MBs.

Employment of the nucleic acid amplification method can substantially increase the signal of MB probes. With HCR amplification (Fig. 9a), Cheglakov *et al.* constructed an amplifier composed of HP1 tagged with Cy3, and HP2 tagged with Cy5 was applied to successfully image miR21 in Hela cells[101]. To image the target miRNA, the miRNA will initiate the alternative assembly between HP1 and HP2, leading to the FRET effect and detection of miRNAs[101]. Using a modified Cascade Hybridization Reaction (CHR, Fig. 9b)[102], Tan and his colleagues improved linear nucleic acid probes and enhanced the signal from *MnSOD* (manganese superoxide dismutase) mRNA by 3.1-fold[103]. As shown in Fig. 9b, the amplification system has three important components: the H1 strand, H2 strand, MB-like dsDNA strand containing a fluorophore and a quencher strand. In the presence of target mRNA, first, the mRNA will catalyse the formation of the H1-H2 hybrid duplex, and then the hybrid duplex will form a complex with the reporter strand and further release the quencher strand, illuminating the location of mRNAs.

Enzyme-mediated signal amplification can also be employed in MBs to increase sensitivity. Zhang *et al.* designed an amplifier (named catalyst-oligomer-mediated enzymatic amplification, CMEA), which contained DNA1, protector-oligomer duplex and catalyst-oligomer as well as NEase (Fig. 10)[104]. In the system, the target miRNA act as the catalyst and one miRNA can create thousands of fluorescent duplexes, allowing detection in the femtomolar range[104]. However, MBs cannot be used directly in live cell RNA imaging since MBs are coated with negatively charged DNA or RNA molecules and cannot automatically enter live cells. To enable live-cell imaging of RNAs by MBs, gene carriers are needed to deliver MBs into cells. The most common MB carriers are cationic liposomes and cationic polymers, e.g., the commercial transfecting agents, Lipofectamine and jetPEI. With transfecting agent, MBs[105] and colour tunable MB-like dsDNAs[106] successfully imaged miR-124a and miR-294 in P19 cells, respectively. Similarly, two types of MBs were simultaneously administered with transfecting agent, realizing simultaneous imaging of miR-26a and miR-206 in C2C12 cells, both *in vitro* and *in vivo*[107]. Kim *et al.* applied hyaluronic acid-targeting liposomes to deliver MB-like dsDNA probes and successfully imaged miR-34a in both primary and metastatic breast cancer cells[97]. Cationic NPs named cationic shell cross-linked knedel-like nanoparticles (cSCK) were also used to deliver PNA-DNA MBs, which successfully imaged iNOS mRNA expression in live mouse macrophage cells[108].

Other nanoparticles can also act as MB carriers. Organic PLGA (poly(D,L-lactide-co-glycolide)) nanoparticles can be applied to deliver MBs, which successfully monitor *β-actin* mRNA expression in mesenchymal stem cells cultured on a 3D matrix[109]. Mesoporous silica nanoparticles (MSNs) were used to load MB-like dsDNAs with CHR amplifiers and successfully imaged miR-21 in live cells[110]. Quantum dots (QDs) loaded R9 peptides and MBs[111] imaged miR-124 in C6 cells and differentiated P19 cells. Furthermore, carbon nanodots (C-dots) loaded dsDNAs[112] imaged miR-124 with high specificity in differentiated

P19 cells. In addition, cationic GNPs loaded HCR components through electrostatic interaction had very high sensitivity due to HCR amplification and were used to track *survivin* mRNAs in Hela cells treated with varying concentrations of a survivin expression repressor, YM155[113].

Cell penetrating peptides and special DNA structures can also act as MB carriers. For instance, TAT peptide conjugated MBs were shown to image *survivin* mRNA in MiaPaca-2 cells after only 60 min of transfection,[114] much faster than conventional robust gene transfection agents (such as lipofectamine) which generally take 3–4 h. Photo-controlled DNA aptamer conjugated MB-like dsDNAs imaged *MnSOD* mRNA in MCF-7 cells with high spatial resolution, in which the aptamers were released from MBs in cells after light activation[115]. DNA aptamers conjugated with MB-like long dsDNAs with multiple fluorophores/quenchers successfully imaged miR-34a in MCF-7 cells, in which the aptamers were released from MBs in cells after target RNA binding[116]. DNA tetrahedron conjugated MBs were also shown to successfully image GAPDH mRNA in DLD-1 and SW480 cells[117]. Moreover, MBs modified with lipid chains can self-assemble into micelles (DNA micelle spherical nucleic acids) and facilitate cell entry. Compared to traditional MBs, DNA micelle SNAs have higher DNA density, stronger binding ability to target RNAs and higher cellular uptake in the absence of transfecting agents[118]. Chen *et al.*[119] synthesized DNA micelle SNAs and used them to image tumour marker *c-raf-1* mRNA with high signal to background ratio.

In all, MBs with stem-loop or dsDNA structures have wide applications in mRNA and miRNA imaging. Backbone modification such as PNA and LNA can greatly lower background signals and enhance MB stability. DNA amplification reactions such as HCR and CHR as well as enzyme-mediated amplification reactions can be used to further enhance MB signals. However, MBs cannot enter cells themselves. For *in vitro* and *in vivo* RNA imaging, gene carriers, such as cationic liposomes, cationic polymers and inorganic NPs, are needed to deliver MBs into cells. In addition, MBs with cell penetrating peptide and DNA aptamer conjugation as well as MB micelles also enable RNA imaging *in vitro* and *in vivo*.

3.3 Nano-MBs

Nano-MBs refer to those NP-loaded MBs in which NPs are incorporated to act as both the quencher and the carrier, and no additional gene carriers are needed to deliver the probes. The NPs here are not just carriers of MBs, but also act as the quenchers of adjacent fluorophores on MBs.

The most typical Nano-MBs are GNP-Nano-MBs (Fig. 11a)[120], which consist of gold nanoparticles (GNPs) functionalized with a shell of molecular beacons or dsDNAs terminated with a fluorophore. When no target RNAs are present, the fluorophores are quenched by GNPs and the whole probes are non-fluorescent; when target mRNAs are present, the sequence in the loop area form a hybrid duplex with target RNA, and the MBs become straight, pushing the fluorophore to be away from GNPs and be dequenched, illuminating target RNAs. Similarly, for dsDNA loaded GNP-Nano-MBs, probes are non-fluorescent due to the quenching ability of gold nanoparticles in the absence of target RNAs; while in the presence of target RNAs, the single recognition strand will form a hybrid duplex

with target RNAs and release the reporter strand and thus illuminate the location of RNAs. In some cases, to better track RNAs in real-time, the reporter strand is designed to be complementary to target RNAs[103, 121–123], such that the fluorophores will be conjugated to target RNAs and able to track target RNAs more accurately. With the reporter strand designed to be complementary to target RNAs, GNP-Nano-MBs (named sticky flares) can quantify the expression of target RNAs and track the spatial distribution of target RNAs[123]. In addition, with FRET probes instead of single fluorophores conjugated on GNPs, the GNP-Nano-MBs would have less false-positive signals[124].

GNP-Nano-MBs were initially applied to image single types of RNAs. For instance, GNP-Nano-MBs were applied to image *survivin* mRNA in SKOV3 cells[125] and *TAT5B* mRNA in MCF-7 cells[126]. Since GNP-Nano-MBs have low background and high sensitivity, they can also image miRNAs with weak binding and low copy numbers. Tu *et al.*[127] applied GNP-Nano-MBs tagged with FITC to detect miR-122 with detection limits as low as 0.01 pM in cell extracts. Since gold nanorods (GNRs) based nano-MBs have almost double signal-to-background ratio of spherical GNP-Nano-MBs,[128] they can be used to track *Dll4* mRNA in HUVEC cells as well as different tissues[128] and the location and expression of heat shock mRNAs (*HSP70* mRNA, Fig. 10b)[129].

GNP-Nano-MBs were also capable of simultaneous multiple-RNA imaging since multiple types of MBs tagged with different fluorophores can be easily modified on GNPs. For instance, GNP Nano-MBs loading Cy3-labelled dsDNAs and Cy5-labelled dsDNAs were applied to image *survivin* mRNA and *β-actin* mRNA simultaneously in MCF-7 cells[130]. Using *β-actin* as the internal control, down-regulation of *survivin* mRNA was accurately quantified[130]. Similarly, GNP-Nano-MBs loading three types of dsDNAs tagged with Rh110, Cy3 and Cy5 were applied to image *c-myc* mRNA, *TK1* mRNA and *GalNAc-T* mRNA[131]. In this way, cancer cells MCF-7 and HepG2 can be distinguished from the normal cells, MCF-10A and HL-7702. Furthermore, GNP-Nano-MBs containing four types of MBs labelled with Alexa Fluor 405, Alexa Fluor 488, Cy3 and Cy5 were applied to image four tumour marker mRNAs (*TK1* mRNA, *survivin* mRNA, *c-myc* mRNA and *GalNAc* mRNA) at the same time[132]. However, simultaneous imaging of four markers needs four couples of excitation/emission, which requires multiple lasers or tuneable laser and multiple detectors. To reduce the requirements in fluorescence microscopy for multiple mRNA imaging, a smart GNP-Nano-MB that only needs single excitation/emission to detect two mRNAs at the same time was developed[133]. In their study, GNPs were conjugated with two types of MBs labelled with Alexa-Fluo 488 and Cy3, which have FRET effects. Efficient FRET only occurs in the presence of both target mRNAs, and the effect can be easily detected by single excitation/emission, *i.e.*, illuminating at the excitation wavelength of the donor and detecting at the emission of the acceptor.

With proper modification, GNP-Nano-MBs can be used for long-time tracking. Choi *et al.* showed that polydopamine (PDA) coated GNPs have much better stability in cells and can track miR-29b and miR-31 (involved in differentiation progress of human mesenchymal stem cells) simultaneously for five days[122]. In detail, they coated polydopamine (PDA) on GNPs and further adsorbed β-hairpin DNA through π-π interactions. In the absence of target miRNAs, the fluorescence of β-hairpin DNA was totally quenched by both GNPs and

PDA, but in the presence of target miRNAs, the β-hairpin DNA detached from the PDA surface and bound with target miRNAs, restoring fluorescence[122].

GNP-Nano-MBs have four advantages: (1) low background signals due to great quenching efficiency to the attached adjacent fluorophores as high as 98% or more[120], which is further due to phase induced radiative energy suppression[134]; (2) excellent resistance to enzyme degradation due to high surface negative charge and high surface salt concentration[135]; (3) high cellular uptake without additional transfecting agents due to special receptor-mediated endocytosis[136]. The probable cellular uptake mechanism is that they target class A scavenger receptors and then enter cells through endocytosis via a lipid-raft-dependent, caveolae-mediated pathway.[136] (4) Enabling additional imaging modality (fluorescence lifetime imaging) due to lengthening of the fluorescence lifetime of Nano-MBs upon binding of target RNAs[137]. On the other hand, it is worth mentioning that in some cases, GNP-Nano-MBs also lead to mRNA downregulation. Since the probes bind to target mRNAs stably through complementary interaction, higher doses of probes (5 nM and 50 nM) and longer incubation time (4 days) leads to RNA downregulation.[125, 138, 139] Therefore, to avoid mRNA deregulation, probes generally have low doses (1 nM) and are incubated with cells for a relatively short time (4 h) in most RNA imaging studies.

In addition to GNPs, other NPs that can quench fluorescence of organic dyes can also be similarly applied to construct nano-MBs. For example, metal-organic framework (MOF) based nano-MBs were applied to detect *Ebola* mRNA on a chip[140]. Polypyrrole nanosphere based nano-MBs were applied to image *TK1* and *c-myc* mRNA in cells[141]. Polydopamine-coated Fe_3O_4 NPs were also applied to image *TK1* and *c-myc* mRNA in cells[142]. However, these newly developed nano-MBs are less sensitive than GNP-Nano-MBs and require optimization for effective RNA imaging.

3.4 Quencher-free probes

Unlike MBs and Nano-MBs, quencher-free probes do not need quenchers to reduce the initial background fluorescence of probes. Instead, the fluorophores in these quencher-free probes are quenched by themselves. FIT probes and ECHO probes are typical quencher-free probes.

An FIT (single dye forced intercalation) probe is generally a ssDNA that contains a single thiazole orange (TO) intercalator serving as an artificial fluorescent nucleobase, which is non-fluorescent at the ssDNA state and becomes fluorescent after forming a duplex with a target RNA (Fig. 11a). Kummer *et al.*[143] used a PNA-FIT probe to image Influenza H1N1 mRNA, and the fluorescence of the probe increased 11-fold in the absence of the target RNAs, while that of the control MB probe targeting the same RNA only increased 6-fold. The high fluorescence increase is attributed to the properties of TO in the probe as well as the PNA structures, which have higher affinity and better biostability than common DNA structures. LNA-FIT probes also have high fluorescence increase, in which an adjacent locked nucleic acid (LNA) unit serves to introduce a local constraint to TO[144].

Even brighter probes can be developed by incorporating fluorophore intercalators with higher fluorescence emission. For instance, TO/JO-FIT probes, which had a 23-fold

fluorescence increase, were developed by conjugating both a TO and more highly emissive fluorophore JO (oxazolopyridine analogue) in a single ssDNA[145]. In the TO/JO-FIT probes, the TO serves as a light collector and transfers the energy to the JO emitter, leading to the successful imaging of *oskar* mRNA within a complex tissue. Similarly, even brighter LNA-QB probes containing QB (quinoline blue) as the intercalator have a 152-fold fluorescence increase[146]. Further combination with LNA-TO probes allows the detection of *oskar* mRNA and total mRNA in oocytes of Drosophila melanogaster by means of the wash-free FISH procedure[146].

Unlike fluorophores (TO/JO/QB) applied in FIT probes, there are some fluorophores that are non-fluorescent in duplexes and fluorescent in ssDNA structures. These fluorophores can also be applied to construct quencher-free probes. Recently, Liao *et al.* developed a quencher-free dsDNA-structured probe containing the 2-aminopurine (2-AP) fluorophore, which can release fluorescent 2-AP-conjugated ssDNA upon binding to target miRNA, leading to the detection limit of target miRNA as low as 5 nM[147].

Further improvement of FIT probes leads to the development of ECHO probes. An ECHO (exciton-controlled hybridization-sensitive fluorescent oligonucleotide) probe is a ssDNA containing two same fluorophores serving as artificial fluorescent nucleobases (Fig. 11b)[148]. In a typical ECHO probe named D514[149] (with maximum absorption at about 514 nm), two TOs are positioned to be parallel (forming H-aggregate) so that the low fluorescence of TOs is quenched (exciton coupling effect) and therefore the background is even lower than that of FIT probes. Then, in the presence of target RNAs, after hybridization of a D514 probe with a target RNA, the parallel state of two TOs is broken and each TO acts independently as an intercalator into a duplex, leading to a 160-fold increase when the target RNA is oligo(A). Later, D514 was successfully applied to image *28S* rRNA and *U3* snoRNA at nucleoli and poly(A) RNA *in vivo*[150].

However, the ECHO probes are not as robust and widely used as FIT probes since the fluorescence increase strongly depends on the sequence of target RNAs. On one hand, ECHO probes are easily subject to self-dimerization; on the other hand, incorporation of LNAs into sites close to dyes even breaks the exciton effect[148].

To this point, we have discussed the structures and principles of four types of endogenous RNA imaging probes: FISH probes, MBs, Nano-MBs and quencher-free probes. FISH probes have the simplest structures and can image thousands of RNAs simultaneously with high sensitivity, but they can only be used to image fixed cells, not live cells. To image RNAs in live cells, the other three types of probes have their distinct advantages. MBs have low background and can image target RNAs with high sensitivity in live cells after signal amplification through DNA amplification or enzyme-mediated amplification methods with the help of different gene carriers. Nano-MBs have even better performance than MBs since the NPs are not only excellent gene carriers, but also great quenchers, and the most typical Nano-MBs are GNP-Nano-MBs, which have been well-studied to image RNAs *in vitro* and *in vivo*. Quencher-free probes utilize special fluorophores that show great fluorescence enhancement in the presence of target RNAs. They have simple structures but high sensitivity and specificity. Typical quencher-free probes include FIT probes and ECHO

probes, with the former type being more versatile and promising for future RNA imaging applications.

There are some other high-performance endogenous RNA imaging probes with more complicated designs. Pumilio homology domain (PUMHD) based BiFC systems can directly image endogenous RNAs since the PUMHD with different structures[151] can be designed according to the target sequences. Tilsner *et al.*[152] fused PUMHD3794 and PUMHD3809 to N- or C-terminal halves of split mCitrine and successfully imaged the genomic RNA of the *tobacco mosaic virus* (TMV). Yamada *et al.* fused PUM3 and PUM4 to N- and C-eGFP and imaged *β-actin* mRNA[1]. Yoshimura *et al.*[43] fused PUM1 and PUM2 to N- and C-eGFP and also successfully imaged *β-actin* mRNA. Yamada *et al.*[153] developed a PUMHD-based BiFC probe to image telomeric repeat-containing RNA by sandwiching PUMHD between the N-eGFP and C-eGFP gene coding sequence. Furthermore, Adamala *et al.*[154] developed a series of programmable RNA-binding protein PumHD, allowing convenient application of the PUMHD-based BiFC system. Similarly, the split RNA aptamer/fluorophore system can also directly image endogenous RNAs[155]. By splitting the Spinach aptamer into two parts (SSA_m and SSA_f) and tagging them with sequences complementary to target RNA sequences, the split Spinach-DFHBI not only has lower background fluorescence, but can also directly image endogenous RNAs through base-pairing[155]. By splitting the Spinach aptamer into two parts and conjugating them to different parts of the RNA, the kinetics of the RNA assembly can be successfully tracked[156]. With the small molecule probe, they successfully imaged *β-actin* mRNA and visualized the cellular dynamics of several endogenous mRNAs including arfaptin-2, cortactin and cytoplasmic FMR1-interacting protein 2. Sato *et al.*[157] utilized a modified RNA aptamer/fluorophore system, by combining a *β-actin* gene-specific RNA aptamer with a cell-permeable synthetic small molecule (BHQ-fluorophore), to image *β-actin* mRNA. The fluorescence of the fluorophore is restored only when the RNA aptamer hybridizes with its cognitive mRNA.

In addition, there are high-performance RNA imaging probe images of miRNA based on its cleaving function[158]. As shown in Fig. 13b, the ssRNA probe has a rather simple structure and its sequence is complementary to that of target miRNA, with two terminals conjugated with fluorophore and quencher, respectively. In the presence of target miRNAs, the ssRNA probes will be cut and the fluorescence of the tagged fluorophore will be restored, revealing the existence of target miRNAs.

Furthermore, endogenous probe/exogenous probe combination can complement each other and offer more imaging information. For instance, Kang *et al.*[159] applied a reporter gene system (CMV/Gluc/3×PT_miR-1) and a miR-1 MB to image miR-1 during myogenesis. The reporter gene system and the miR-1 MB imaged miR-1 indirectly and directly, respectively.

4. RNA imaging applications

4.1 Applications in tracking RNA processes

Table 1 shows the application in tracking RNA processes by RNA imaging probes. Generally, two important processes are tracked: (1) processes during formation and translation of mRNAs; (2) biogenesis of miRNAs.

The mRNA processes generally include transcription, localization, transport, and translation[4, 21]. By tracking nascent RNAs, it was revealed that strongly expressed housekeeping genes alter the magnitude of their transcriptional pulses during development by the RBP-FP system[160]. By tracking pre-mRNA with a RBP-FP system, a kinetic description for spliceosome assembly was monitored in live cells[161]. By labelling exons and introns of GFP pre-mRNA with two distinct sets of FISH probes[162], splicing events were visualized with single molecule sensitivity. It was revealed that tight coupling between transcription and splicing can be broken when the intron's polypyrimidine tract is sequestered within strong secondary structures. Among all mRNAs, *β-actin* mRNA is one of the most studied mRNAs for RNA processes. For transcription, the rates of transcription initiation and termination of FISH probe labelled *β-actin* mRNA were determined by positioning probes along the transcription unit[77]; the transcriptional bursting of *β-actin* mRNAs in response to serum stimulation and their transport in primary live cells were visualized by the BiFC system[43]; the transportation dynamics of single *β-actin* mRNA particles in primary hippocampal neurons was clearly tracked by the RBP-FP system[35]. For localization and transport, co-localization of *β-actin* mRNA with microtubules were localized predominantly by diffusion in primary fibroblasts; however, multiple *β-actin* mRNAs can assemble together (Fig. 13A) and travel by active transport and disassemble upon depolarization by potassium chloride by the RBP-FP system (Fig. 13B–G)[36]. Real-time transport of *β-actin* mRNA in mouse embryonic fibroblasts was monitored by GNP-Nano-MB[123]. For translation, the unmasking of the FISH probe labelled *β-actin* mRNA during translation was found to be prompted by chemically induced long-term potentiation, which was further controlled by synaptic activity (Fig. 13)[163].

In addition to *β-actin* mRNAs, the processes of some other mRNAs were also studied using RNA imaging probes. The localization of *gurken* mRNA in developing Drosophila oocytes was found to be affected by nine complementation groups of gene sequences and the localization occurred before centrosome localization[165]. For transport, the feasibility of tracking the transport of *c-myc* mRNA was demonstrated in heated cells[166]; *oskar* mRNA particles in living oocytes were found to be actively transported along microtubules in all directions with a slight bias toward the posterior[167]; the transport of a model mRNA transcript in body wall muscle cells was tracked in transgenic *Drosophila*, revealing that myofibers are compartmentalized and consist of domains[168].

Choosing proper imaging probes for tracking mRNA processes is important for successful dynamic mRNA imaging. From Table 1, it can be seen that the RBP-FP system is the most widely used probe for tracking mRNA processes, while the BiFC system and FISH probe are also candidates for tracking mRNA processes. However, fast transcription kinetics can only be monitored by the RBP-FP system. The RBP-FP system is simple and particularly convenient for labelling a common mRNA in the 3′-UTR. Moreover, the RBP-FP system is very stable due to the fact that the FP is stably bound to the target mRNA. Therefore, RBP-FP is one of the most suitable probes for the real-time tracking of model mRNA processes. However, for the BiFC system, it takes time to image target RNAs and it is not suitable for real-time imaging of fast processes. For the FISH probe, the sample preparation takes time, and therefore it is not suitable for tracking fast processes either. Specifically, Wang *et al.* synthesized an activatable GNP-MB (fNC) that can activate the transcription of *Tubb3*

mRNA and *Fox3* mRNA and image the process (Fig. 15)[164]. Since the process is not so fast, the dynamics can be tracked by Nano-MBs. On the other hand, RNA imaging probes can also be applied to track miRNA biogenesis during different physiological processes. The most studied processes are neurogenesis and myogenesis. Neurogenesis includes neuronal proliferation and differentiation. The miR-124a was found to have higher expression during neurogenesis by MB[112]. Furthermore, the biogenesis of the same miRNA during neuronal differentiation was successfully detected by the reporter gene system[70] or MB[105, 111]. In addition to miR-124a, the miR-1a[106] and miR-23a[73] were also found to increase expression during neuronal differentiation by MB[106] and the reporter gene system[73], respectively. Similarly, miR-1, miR-26a and miR206 were found to increase expression during myogenesis by applying RNA imaging probes. Furthermore, miR221 was found to increase expression in papillary thyroid carcinoma by the reporter gene system[68].

Strategies for successful dynamic miRNA imaging are different from those of mRNA since the structure and function of miRNA is quite different from that of mRNA. As for the structure of miRNA, it is very short, only 21–25 nt and therefore has much weaker binding to probes than mRNAs. Moreover, the expression of miRNAs is much lower than that of mRNAs. The short length and low copy number of miRNAs require that the imaging probes have high binding affinity and high sensitivity. MB is quite suitable for imaging miRNA, since it has low background and high binding affinity to miRNAs. With proper amplification methods, MB has even higher sensitivity. FISH probes also have very high binding affinity and high sensitivity, but they are not suitable for imaging miRNA biogenesis. The reason could be that they cannot be used in live cell imaging and cannot track fast biogenesis. Furthermore, miRNA can regulate related genes by binding to the gene control region. The reporter gene system specifically utilizes this principle and substantially increases the detection sensitivity. Therefore, the most suitable miRNA probes are MB and the reporter gene system.

In summary, the requirements for dynamic mRNA imaging and miRNA imaging are quite different. For dynamic mRNA imaging, the probes should be able to track the fast mRNA processes, and the requirements include the following: (1) the probes should have high resolution; (2) the probes can track mRNA in real-time; (3) the probes should be stably bound to target mRNA. For dynamic miRNA imaging, due to its regulatory function, the reporter gene system is a good choice for its indirect detection. For direct dynamic miRNA imaging, the probes should be able to bind to low-copy-number and low-expression miRNA with high efficiency, and the most important requirement is that the probe should have very high resolution.

4.2 Applications in cancer diagnosis

Table 2 summarizes mRNA and miRNA tumour markers detected by RNA imaging probes. The mRNA and miRNA tumour markers have high expression in certain tumour cells, but have low expression in normal cells; therefore, detection and quantification of the mRNA or miRNA tumour markers can help in cancer diagnosis.

For the detection of single mRNA tumour markers, both MB and Nano-MBs have been successfully applied in detecting *survivin* mRNA[113, 114, 125, 130], *MnSOD* mRNA[103, 115], *c*-

raf-1 mRNA[119], *TK1* mRNA[124], *STAT5B* mRNA[126] and *K-ras* mRNA[170] in different tumour cells.

Multiple mRNA tumour marker detection can improve the accuracy of cancer detection, which can be easily accomplished by Nano-MBs. The *TK1* mRNA and *GalNAc* mRNA were imaged at the same time, distinguishing cancer cells (MCF-7 and HepG2 cells) from normal cells by GNP-Nano-MB[121]. Similarly, simultaneous imaging of another two mRNAs (*c-myc*/*TK1* mRNA[141, 142], *TK1*/*survivin* mRNA[133]), three mRNAs (c-myc/*TK1*/*GalNac-T* mRNA[131]) and even four mRNAs (Fig. 16, *c-myc*/*TK1*/*GalNac-T*/*survivin* mRNA[132]), which increase the accuracy of cancer diagnosis, can also be accomplished by Nano-MB.

Looking into the probes for detection of mRNA tumour markers, almost all the probes are MB based: MB or Nano-MB. The reason could be that the mRNA tumour markers have many types and the sequences of tumour markers are quite different for each. MB has a simple structure and can be easily designed to bind to different tumour markers with high binding affinity. Nano-MB further increases its cellular delivery efficiency and imaging sensitivity and is therefore suitable for mRNA tumour marker detection.

In addition to mRNA tumour markers, miRNA tumour markers can also be used in cancer diagnosis. However, the short length and low copy number of miRNAs make them even harder to detect than mRNA tumour markers, and therefore, miRNA imaging probes have higher sensitivity than that of mRNA imaging probes. Generally, there are four types of highly-sensitive miRNA imaging probes: MBs with signal amplification, nano-MBs, FISH probes and reporter gene systems. For instance, miR-21[101, 110], *let-7a* miRNA[87, 104] and miR-34a[116] can all be detected by MBs with amplification methods. miR-122 from human Huh7 cells can be accurately detected by GNP-Nano-MB[127]. The miRNAs (miR15a[11], miR155[11] and miR-21[5]) in different tumour environments can be detected by enhanced LNA FISH probes with[11] or without[5] amplification methods. The miR22[67] from A549 cells and miR16[74] from chemoresistant SGC7901/VCR cells as well as miR16[74] from xenografts were detected by reporter gene systems (Fig. 17). In addition, miRNA itself has the special property that it can cut its bound RNA sequences. Based on this property, miR-10 from MDA-MB-231 cells can be detected by the designed ssRNA probe[158].

To realize early and accurate cancer diagnosis through the detection of mRNA or miRNA tumour markers, the RNA imaging probes should at least meet the following three requirements: (1) the probes should have high specificity in distinguishing tumour markers from RNAs with similar sequences; (2) the probes should have high resolution or sensitivity in detecting low expression of mRNA or miRNA tumour markers; (3) the probes should have high versatility to be applicable to a wide range of tumour markers.

Conclusions and Outlook

RNA imaging is very important in two aspects. Firstly, RNA imaging can track RNA processes such as transcription, localization, transport and translation, and can also track the biogenesis of miRNAs. Secondly, RNA imaging can be used in cancer diagnosis, since

certain mRNAs or miRNAs can act as tumour markers. However, RNA imaging is at present mostly at the cellular level; *in vivo* imaging is very rare.

In this review, we summarized current high-performance RNA imaging probes, analysed their structures and imaging principles, and correlated the designs with their applications, which may offer guidance for future optimization of current probes. Generally, we reached the following conclusions:

- All RNAs can be imaged using RNA probes designed based on base-pairing principles since all RNAs share similar chemical structures.
- The mRNAs can accommodate RNA aptamers or special protein-binding RNAs in their non-coding 3′-UTRs, which can further bind to fluorescent proteins or small molecular dyes. Based on these principles, single-molecule mRNA can be imaged using RBP-FP, BiFC and RNA aptamer/fluorophore systems.
- The microRNAs have special properties that regulate corresponding mRNAs; therefore, the reporter-gene system is applicable for miRNA imaging. Also, miRNAs can cut their binding RNAs, leading to the more simple design of ssRNA probes.
- MBs have simple structures and high specificity and are suitable for the detection of a wide range of mRNA and miRNA. Nano-MBs are more advantageous than MBs. Among them, GNP based Nano-MBs are the most robust and versatile RNA imaging probes for live-cell RNA imaging.
- FISH probes have high sensitivity, but can only image RNAs in fixed cells, and are therefore often used to image relatively slow RNA processes or detect low-content tumour miRNAs.
- Quencher-free probes have very simple structures, but they are not as versatile as MBs and are therefore less applied in live-cell RNA imaging. Further improvement in specificity can push quencher-free probes into RNA imaging *in vitro* and *in vivo*.

To optimize the efficacy of current RNA imaging probes, there are three possible solutions. First, we can use nucleic acid probes with chemical modifications, such as LNA. Second, we can develop more excellent gene carriers, which not only deliver probes with high efficiency, but also act as high-performance fluorescence quenchers, such as GNP with porous structures. Third, we can chemically modify current fluorophores[171] so that they have higher OFF/ON signal enhancement upon binding of target RNAs. In addition, optimization of imaging equipment[172] and mathematical methods[173, 174] can further improve RNA imaging resolution.

Acknowledgments

This study was supported in part by the National Natural Science Foundation of China (Nos. 81671753 and 81501524), the national 1000 Young Talents Program of China, the Fundamental Research Funds for the Central universities under No. JB161202, and the Intramural Research Program, National Institute of Biomedical Imaging and Bioengineering (NIBIB), National Institutes of Health (NIH).

References

1. Yamada T, Yoshimura H, Inaguma A, Ozawa T. Analytical Chemistry. 2011; 83:5708–5714. [PubMed: 21634804]
2. Ke R, Mignardi M, Pacureanu A, Svedlund J, Botling J, Wahlby C, Nilsson M. Nature Methods. 2013; 10:857–862. [PubMed: 23852452]
3. Darnell DK, Stanislaw S, Kaur S, Antin PB. RNA. 2010; 16:632–637. [PubMed: 20086052]
4. Buxbaum AR, Yoon YJ, Singer RH, Park HY. Trends in cell biology. 2015; 25:468–475. [PubMed: 26052005]
5. Sempere LF, Korc M. Pancreatic Cancer: Methods and Protocols. 2013:43–59.
6. Lee K, Cui Y, Lee LP, Irudayaraj J. Nature Nanotechnology. 2014; 9:474–480.
7. Weil TT, Parton RM, Davis I. Trends in Cell Biology. 2010; 20:380–390. [PubMed: 20444605]
8. Rodriguez AJ, Condeelis J, Singer RH, Dictenberg JB. Seminars in Cell & Developmental Biology. 2007:18, 202–208.
9. Chao JA, Yoon YJ, Singer RH. Cold Spring Harbor Perspectives in Biology. 2012; 4:a012310. [PubMed: 22960595]
10. Silahtaroglu AN, Nolting D, Dyrskjøt L, Berezikov E, Møller M, Tommerup N, Kauppinen S. Nature protocols. 2007; 2:2520–2528. [PubMed: 17947994]
11. Lu J, Tsourkas A. Nucleic acids research. 2009; 37:e100–e100. [PubMed: 19515934]
12. Chao J, Cao W, Su S, Weng L, Song S, Fan C, Wang L. Journal of Materials Chemistry B. 2016; 4:1757–1769.
13. Abell JL, Garren JM, Driskell JD, Tripp RA, Zhao Y. Journal of the American Chemical Society. 2012; 134:12889–12892. [PubMed: 22788749]
14. Bell SEJ, Sirimuthu NMS. Journal of the American Chemical Society. 2006; 128:15580–15581. [PubMed: 17147354]
15. Driskell JD, Tripp RA. Chemical Communications. 2010; 46:3298–3300. [PubMed: 20442892]
16. Kim S, Park JE, Hwang W, Seo J, Lee YK, Hwang JH, Nam JM. Journal of the American Chemical Society. 2017; doi: 10.1021/jacs.7b01311
17. Guven B, Dudak FC, Boyaci IH, Tamer U, Ozsoz M. Analyst. 2014; 139:1141–1147. [PubMed: 24418951]
18. Ye L-P, Hu J, Liang L, Zhang C-y. Chemical Communications. 2014; 50:11883–11886. [PubMed: 25154520]
19. Lee H, Park JE, Nam JM. Nature Communications. 2014; 5:3367.
20. Kelley SO, Mirkin CA, Walt DR, Ismagilov RF, Toner M, Sargent EH. Nature nanotechnology. 2014; 9:969–980.
21. Tyagi S. Nature Methods. 2009; 6:331–338. [PubMed: 19404252]
22. Santangelo, PJ., Alonas, E., Jung, J., Lifland, AW., Zurla, C. Methods in Enzymology, Vol 505: Imaging and Spectroscopic Analysis of Living Cells: Live Cell Imaging of Cellular Elements and Functions. Conn, PM., Elsvier Inc. , editor. Vol. 505. 2012. p. 383-399.
23. Rath AK, Rentmeister A. Current opinion in biotechnology. 2015; 31:42–49. [PubMed: 25173610]
24. Rhee WJ, Bao G. BMC biotechnology. 2009; 9:30. [PubMed: 19341452]
25. Li Q, Liu L, Liu JW, Jiang JH, Yu RQ, Chu X. TrAC Trends in Analytical Chemistry. 2014; 58:130–144.
26. Hayashi G, Okamoto A. Chemical Record. 2013; 13:209–217. [PubMed: 23495145]
27. Boutorine AS, Novopashina DS, Krasheninina OA, Nozeret K, Venyaminova AG. Molecules. 2013; 18:15357–15397. [PubMed: 24335616]
28. Zhang P, Cheetham AG, Lock LL, Li Y, Cui H. Current opinion in biotechnology. 2015; 34:171–179. [PubMed: 25687686]
29. Thomas JA. Chemical Society Reviews. 2015; 44:4494–4500. [PubMed: 26130212]
30. Meng HM, Liu H, Kuai H, Peng R, Mo L, Zhang XB. Chemical Society Reviews. 2016; 45:2583–2602. [PubMed: 26954935]

31. Heuer-Jungemann A, Harimech PK, Brown T, Kanaras AG. Nanoscale. 2013; 5:9503–9510. [PubMed: 23982570]
32. Wang F, Niu G, Chen X, Cao F. European Journal of Nuclear Medicine and Molecular Imaging. 2011; 38:1572–1579. [PubMed: 21448701]
33. Urbanek MO, Nawrocka AU, Krzyzosiak WJ. International journal of molecular sciences. 2015; 16:13259–13286. [PubMed: 26068454]
34. Bertrand E, Chartrand P, Schaefer M, Shenoy SM, Singer RH, Long RM. Molecular cell. 1998; 2:437–445. [PubMed: 9809065]
35. Lionnet T, Czaplinski K, Darzacq X, Shav-Tal Y, Wells AL, Chao JA, Park HY, de Turris V, Lopez-Jones M, Singer RH. Nature Methods. 2011; 8:165–170. [PubMed: 21240280]
36. Park HY, Lim H, Yoon YJ, Follenzi A, Nwokafor C, Lopez-Jones M, Meng X, Singer RH. Science. 2014; 343:422–424. [PubMed: 24458643]
37. Carrocci TJ, Hoskins AA. Analyst. 2014; 139:44–47. [PubMed: 24187681]
38. Valencia-Burton M, Broude NE. Current protocols in cell biology/editorial board, Juan S Bonifacino … [et al]. 2007 Chapter 17, Unit 17.11-Unit 17.11.
39. Hocine S, Raymond P, Zenklusen D, Chao JA, Singer RH. Nature methods. 2013; 10:119–121. [PubMed: 23263691]
40. Wu B, Chao JA, Singer RH. Biophysical Journal. 2012; 102:2936–2944. [PubMed: 22735544]
41. Hu CD, Chinenov Y, Kerppola TK. Molecular cell. 2002; 9:789–798. [PubMed: 11983170]
42. Kodama Y, Hu CD. BioTechniques. 2012; 53:285–298. [PubMed: 23148879]
43. Yoshimura H, Inaguma A, Yamada T, Ozawa T. ACS chemical biology. 2012; 7:999–1005. [PubMed: 22387832]
44. Dictenberg J. Trends in Biotechnology. 2012; 30:621–626. [PubMed: 23127753]
45. Wu B, Chen J, Singer RH. Scientific Reports. 2014; 4:3615. [PubMed: 24402470]
46. Yiu HW, Demidov VV, Toran P, Cantor CR, Broude NE. Pharmaceuticals. 2011; 4:494–508.
47. Paige JS, Wu KY, Jaffrey SR. Science. 2011; 333:642–646. [PubMed: 21798953]
48. Zhang J, Fei J, Leslie BJ, Han KY, Kuhlman TE, Ha T. Scientific reports. 2015; 5:17295. [PubMed: 26612428]
49. Strack RL, Disney MD, Jaffrey SR. Nature Methods. 2013; 10:1219–1227. [PubMed: 24162923]
50. You M, Jaffrey SR. Annual review of biophysics. 2015; 44:187–206.
51. Warner KD, Chen MC, Song W, Strack RL, Thorn A, Jaffrey SR, Ferré-D'Amaré AR. Nature structural & molecular biology. 2014; 21:658–663.
52. Filonov GS, Moon JD, Svensen N, Jaffrey SR. Journal of the American Chemical Society. 2014; 136:16299–16308. [PubMed: 25337688]
53. Autour A, Westhof E, Ryckelynck M. Nucleic acids research. 2016; 44:2491–2500. [PubMed: 26932363]
54. Sunbul M, Jäschke A. Angewandte Chemie International Edition. 2013; 52:13401–13404. [PubMed: 24133044]
55. Arora A, Sunbul M, Jäschke A. Nucleic acids research. 2015; 43:e144–e144. [PubMed: 26175046]
56. Dolgosheina EV, Jeng SC, Panchapakesan SSS, Cojocaru R, Chen PS, Wilson PD, Hawkins N, Wiggins PA, Unrau PJ. ACS chemical biology. 2014; 9:2412–2420. [PubMed: 25101481]
57. Song W, Strack RL, Svensen N, Jaffrey SR. Journal of the American Chemical Society. 2014; 136:1198–1201. [PubMed: 24393009]
58. Ilgu M, Ray J, Bendickson L, Wang T, Geraskin IM, Kraus GA, Nilsen-Hamilton M. Methods. 2016; 98:26–33. [PubMed: 26707205]
59. Shin I, Ray J, Gupta V, Ilgu M, Beasley J, Bendickson L, Mehanovic S, Kraus GA, Nilsen-Hamilton M. Nucleic Acids Research. 2014; 42:e90. [PubMed: 24753407]
60. Kim S, Hwang DW, Lee DS. FEBS journal. 2009; 276:2165–2174. [PubMed: 19250311]
61. Niu G, Chen X. Molecular Imaging and Biology. 2009; 11:61–63. [PubMed: 19037611]
62. Niu G, Chen X. Theranostics. 2012; 2:413–423. [PubMed: 22539937]
63. Oh SW, Do Won Hwang DSL. Theranostics. 2013; 3:1004. [PubMed: 24396509]

64. Pillai RS. Rna-a Publication of the Rna Society. 2005; 11:1753–1761.
65. Dong H, Lei J, Ding L, Wen Y, Ju H, Zhang X. Chemical reviews. 2013; 113:6207–6233. [PubMed: 23697835]
66. Choi Y, Do won Hwang MYK, Kim JY, Sun W, Lee DS. Frontiers in Molecular Neuroscience. 2016; 9:52. [PubMed: 27462205]
67. Wang F, Zhang B, Zhou L, Shi Y, Li Z, Xia Y, Tian J. ACS applied materials & interfaces. 2016; 8:9014–9021. [PubMed: 27010367]
68. Kim HJ, Chung JK, Lee DS, Kim S. Molecular Imaging and Biology. 2009; 11:71–78. [PubMed: 19030936]
69. Tu Y, Wan L, Zhao D, Bu L, Dong D, Yin Z, Cheng Z, Shen B. European journal of nuclear medicine and molecular imaging. 2014; 41:972–984. [PubMed: 24504502]
70. Ko HY, Lee DS, Kim S. Nature protocols. 2009; 4:1663–1669. [PubMed: 19876026]
71. Ko HY, Lee YS, Kim S. Bioluminescent Imaging: Methods and Protocols. 2014:85–95.
72. Troy T, Jekic-McMullen D, Sambucetti L, Rice B. Molecular imaging. 2004; 3:9–23. [PubMed: 15142408]
73. Lee JY, Kim S, Jeong JM, Chung JK, Lee MC, Lee DS. Journal of nuclear medicine. 2008; 49:285–294. [PubMed: 18199619]
74. Wang F, Song X, Li X, Xin J, Wang S, Yang W, Wang J, Wu K, Chen X, Liang J. PloS one. 2013; 8:e61792. [PubMed: 23613938]
75. Levsky JM, Singer RH. Journal of Cell Science. 2003; 116:2833–2838. [PubMed: 12808017]
76. Huang J, Wang H, Yang X, Quan K, Yang Y, Ying L, Xie N, Ou M, Wang K. Chemical Science. 2016; 7:3829–3835.
77. Femino AM, Fay FS, Fogarty K, Singer RH. Science. 1998; 280:585–590. [PubMed: 9554849]
78. Trcek T, Chao JA, Larson DR, Park HY, Zenklusen D, Shenoy SM, Singer RH. Nature Protocols. 2012; 7:408–419. [PubMed: 22301778]
79. Raj A, Tyagi S. Methods in enzymology. 2010; 472:365–386. [PubMed: 20580972]
80. Kwon S. Bmb Reports. 2013; 46:65–72. [PubMed: 23433107]
81. Vautrot V, Aigueperse C, Branlant C, Behm-Ansmant I. Small Non-Coding RNAs: Methods and Protocols. 2015:73–83.
82. Li J, Li X, Li Y, Yang H, Wang L, Qin Y, Liu H, Fu L, Guan XY. PloS one. 2013; 8:e53582. [PubMed: 23301089]
83. Song R, Ro S, Yan W. RNA Therapeutics: Function, Design, and Delivery. 2010:285–292.
84. Søe MJ, Møller T, Dufva M, Holmstrøm K. Journal of Histochemistry & Cytochemistry. 2011; 59:661–672. [PubMed: 21525189]
85. Choi HM, Chang JY, Trinh LA, Padilla JE, Fraser SE, Pierce NA. Nature biotechnology. 2010; 28:1208–1212.
86. Ge J, Zhang LL, Liu SJ, Yu RQ, Chu X. Analytical chemistry. 2014; 86:1808–1815. [PubMed: 24417222]
87. Deng R, Tang L, Tian Q, Wang Y, Lin L, Li J. Angewandte Chemie International Edition. 2014; 53:2389–2393. [PubMed: 24469913]
88. Chaudhuri AD, Yelamanchili SV, Fox HS. Frontiers in cellular neuroscience. 2013; 7:1–8. [PubMed: 23355802]
89. Wang Z, Yang B. MicroRNA Expression Detection Methods, Springer. 2010:353–359.
90. Paragas VB, Zhang YZ, Haugland RP, Singer VL. Journal of Histochemistry & Cytochemistry. 1997; 45:345–357. [PubMed: 9071316]
91. Lubeck E, Coskun AF, Zhiyentayev T, Ahmad M, Cai L. Nature Methods. 2014; 11:360–361. [PubMed: 24681720]
92. Chen KH, Boettiger AN, Moffitt JR, Wang S, Zhuang X. Science. 2015; 348:aaa6090. [PubMed: 25858977]
93. Wu CS, Peng L, You M, Han D, Chen T, Williams KR, Yang CJ, Tan W. International journal of molecular imaging. 2012; 2012:501579–501579. [PubMed: 23209893]

94. Yang CYJ, Medley CD, Tan WH. Current Pharmaceutical Biotechnology. 2005; 6:445–452. [PubMed: 16375729]
95. Han S, Jia X, Ma J, Zhu Q. Archivum immunologiae et therapiae experimentalis. 2013; 61:139–148. [PubMed: 23292078]
96. Wang K, Tang Z, Yang CJ, Kim Y, Fang X, Li W, Wu Y, Medley CD, Cao Z, Li J. Angewandte Chemie International Edition. 2009; 48:856–870. [PubMed: 19065690]
97. Kim E, Yang J, Park J, Kim S, Kim NH, Yook JI, Suh JS, Haam S, Huh YM. ACS nano. 2012; 6:8525–8535. [PubMed: 22947044]
98. El-Yazbi AF, Loppnow GR. Analytical chemistry. 2013; 85:4321–4327. [PubMed: 23544988]
99. Wu Y, Yang CJ, Moroz LL, Tan W. Analytical Chemistry. 2008; 80:3025–3028. [PubMed: 18321137]
100. Socher E, Bethge L, Knoll A, Jungnick N, Herrmann A, Seitz O. Angewandte Chemie International Edition. 2008; 47:9555–9559. [PubMed: 18949813]
101. Cheglakov Z, Cronin TM, He C, Weizmann Y. Journal of the American Chemical Society. 2015; 137:6116–6119. [PubMed: 25932784]
102. Jung C, Ellington AD. Accounts of chemical research. 2014; 47:1825–1835. [PubMed: 24828239]
103. Wu C, Cansiz S, Zhang L, Teng I, Qiu L, Li J, Liu Y, Zhou C, Hu R, Zhang T. Journal of the American Chemical Society. 2015; 137:4900–4903. [PubMed: 25835750]
104. Zhang K, Wang K, Zhu X, Xie M. Sensors and Actuators B: Chemical. 2016; 223:586–590.
105. Lee J, Kim S. RNA Imaging: Methods and Protocols. 2016:129–138.
106. Kang HJ, Lee J, Ali BA, Al-Khedhairy AA, Kim S. RNA & DISEASE. 2015; 2:e697.
107. Kang WJ, Cho YL, Chae JR, Lee JD, Choi KJ, Kim S. Biomaterials. 2011; 32:1915–1922. [PubMed: 21122913]
108. Wang Z, Zhang K, Shen Y, Smith J, Bloch S, Achilefu S, Wooley KL, Taylor JS. Organic & Biomolecular Chemistry. 2013; 11:3159–3167. [PubMed: 23538604]
109. Wiraja C, Yeo DC, Chew SY, Xu C. Journal of Materials Chemistry B. 2015; 3:6148–6156.
110. Wang Y, Yu Z, Zhang Z, Ren R, Zhang S. Analyst. 2016; 141:2861–2864. [PubMed: 27063644]
111. Lee J, Moon SU, Lee YS, Ali BA, Al-Khedhairy AA, Ali D, Ahmed J, Al Salem AM, Kim S. Sensors. 2015; 15:12872–12883. [PubMed: 26043176]
112. Noh EH, Ko HY, Lee CH, Jeong MS, Chang YW, Kim S. Journal of Materials Chemistry B. 2013; 1:4438–4445.
113. Wu Z, Liu GQ, Yang XL, Jiang JH. Journal of the American Chemical Society. 2015; 137:6829–6836. [PubMed: 25969953]
114. Nitin N, Santangelo PJ, Kim G, Nie S, Bao G. Nucleic acids research. 2004; 32:e58–e58. [PubMed: 15084673]
115. Qiu L, Wu C, You M, Han D, Chen T, Zhu G, Jiang J, Yu R, Tan W. Journal of the American Chemical Society. 2013; 135:12952–12955. [PubMed: 23931073]
116. Kim J, Lee E, Kang YY, Mok H. Chemical Communications. 2015; 51:9038–9041. [PubMed: 25939820]
117. Tay CY, Yuan L, Leong DT. ACS nano. 2015; 9:5609–5617. [PubMed: 25906327]
118. Wang Y, Wu C, Chen T, Sun H, Cansiz S, Zhang L, Cui C, Hou W, Wu Y, Wan S. Chemical Science. 2016; 7:6041–6049. [PubMed: 28066539]
119. Chen T, Wu CS, Jimenez E, Zhu Z, Dajac JG, You M, Han D, Zhang X, Tan W. Angewandte Chemie-International Edition. 2013; 52:2012–2016. [PubMed: 23319350]
120. Dubertret B, Calame M, Libchaber AJ. Nature biotechnology. 2001; 19:365–370.
121. Pan W, Yang H, Li N, Yang L, Tang B. Chemistry–A European Journal. 2015; 21:6070–6073.
122. Choi CKK, Li J, Wei K, Xu YJ, Ho LWC, Zhu M, To KK, Choi CHJ, Bian L. Journal of the American Chemical Society. 2015; 137:7337–7346. [PubMed: 25996312]
123. Briley WE, Bondy MH, Randeria PS, Dupper TJ, Mirkin CA. Proceedings of the National Academy of Sciences. 2015; 112:9591–9595.

124. Yang Y, Huang J, Yang X, Quan K, Wang H, Ying L, Xie N, Ou M, Wang K. Journal of the American Chemical Society. 2015; 137:8340–8343. [PubMed: 26110466]
125. Seferos DS, Giljohann DA, Hill HD, Prigodich AE, Mirkin CA. Journal of the American Chemical Society. 2007; 129:15477–15479. [PubMed: 18034495]
126. Xue J, Shan L, Chen H, Li Y, Zhu H, Deng D, Qian Z, Achilefu S, Gu Y. Biosensors and Bioelectronics. 2013; 41:71–77. [PubMed: 23122230]
127. Tu Y, Wu P, Zhang H, Cai C. Chemical Communications. 2012; 48:10718–10720. [PubMed: 22945460]
128. Wang S, Riahi R, Li N, Zhang DD, Wong PK. Advanced Materials. 2015; 27:6034–6038. [PubMed: 26314800]
129. Riahi R, Wang S, Long M, Li N, Chiou PY, Zhang DD, Wong PK. ACS nano. 2014; 8:3597–3605. [PubMed: 24645754]
130. Prigodich AE, Randeria PS, Briley WE, Kim NJ, Daniel WL, Giljohann DA, Mirkin CA. Analytical Chemistry. 2012; 84:2062–2066. [PubMed: 22288418]
131. Li N, Chang C, Pan W, Tang B. Angewandte Chemie International Edition. 2012; 51:7426–7430. [PubMed: 22806948]
132. Pan W, Zhang T, Yang H, Diao W, Li N, Tang B. Analytical chemistry. 2013; 85:10581–10588. [PubMed: 24088027]
133. Pan W, Li Y, Wang M, Yang H, Li N, Tang B. Chemical Communications. 2016; 52:4569–4572. [PubMed: 26939827]
134. Dulkeith E, Ringler M, Klar T, Feldmann J, Munoz Javier A, Parak W. Nano Letters. 2005; 5:585–589. [PubMed: 15826091]
135. Seferos DS, Prigodich AE, Giljohann DA, Patel PC, Mirkin CA. Nano letters. 2008; 9:308–311.
136. Choi CHJ, Hao L, Narayan SP, Auyeung E, Mirkin CA. Proceedings of the National Academy of Sciences. 2013; 110:7625–7630.
137. Shi J, Zhou M, Gong A, Li Q, Wu Q, Cheng GJ, Yang M, Sun Y. Analytical chemistry. 2016; 88:1979–1983. [PubMed: 26813157]
138. Prigodich AE, Seferos DS, Massich MD, Giljohann DA, Lane BC, Mirkin CA. Acs Nano. 2009; 3:2147–2152. [PubMed: 19702321]
139. Rosi NL, Giljohann DA, Thaxton CS, Lytton-Jean AK, Han MS, Mirkin CA. Science. 2006; 312:1027–1030. [PubMed: 16709779]
140. Qin L, Lin LX, Fang ZP, Yang SP, Qiu GH, Chen JX, Chen WH. Chemical Communications. 2016; 52:132–135. [PubMed: 26502791]
141. Ke K, Lin L, Liang H, Chen X, Han C, Li J, Yang HH. Chemical Communications. 2015; 51:6800–6803. [PubMed: 25786907]
142. Lin L, Cong Z, Cao J, Ke K, Peng Q, Gao J, Yang H, Liu G, Chen X. ACS nano. 2014; 8:3876–3883. [PubMed: 24654734]
143. Kummer S, Knoll A, Socher E, Bethge L, Herrmann A, Seitz O. Angewandte Chemie International Edition. 2011; 50:1931–1934. [PubMed: 21328673]
144. Hövelmann F, Gaspar I, Loibl S, Ermilov EA, Röder B, Wengel J, Ephrussi A, Seitz O. Angewandte Chemie International Edition. 2014; 53:11370–11375. [PubMed: 25167966]
145. Hövelmann F, Gaspar I, Ephrussi A, Seitz O. Journal of the American Chemical Society. 2013; 135:19025–19032. [PubMed: 24295172]
146. Hövelmann F, Gaspar I, Chamiolo J, Kasper M, Steffen J, Ephrussi A, Seitz O. Chemical Science. 2016; 7:128–135.
147. Liao R, He K, Chen C, Chen X, Cai C. Analytical chemistry. 2016; 88:4254–4258. [PubMed: 26985690]
148. Okamoto A. Chemical Society Reviews. 2011; 40:5815–5828. [PubMed: 21660343]
149. Ikeda S, Okamoto A. Chemistry–An Asian Journal. 2008; 3:958–968.
150. Oomoto I, Suzuki-Hirano A, Umeshima H, Han YW, Yanagisawa H, Carlton P, Harada Y, Kengaku M, Okamoto A, Shimogori T, Wang DO. Nucleic Acids Research. 2015; 43:e126. [PubMed: 26101260]

151. Tilsner J. Plasmodesmata: Methods and Protocols. 2015:295–328.
152. Tilsner J, Linnik O, Christensen NM, Bell K, Roberts IM, Lacomme C, Oparka KJ. The Plant Journal. 2009; 57:758–770. [PubMed: 18980643]
153. Yamada T, Yoshimura H, Shimada R, Hattori M, Eguchi M, Fujiwara TK, Kusumi A, Ozawa T. Scientific Reports. 2016; 6:38910. [PubMed: 27958374]
154. Adamala KP, Martin-Alarcon DA, Boyden ES. Proceedings of the National Academy of Sciences. 2016; 113:E2579–E2588.
155. Kikuchi N, Kolpashchikov DM. Chem Bio Chem. 2016; 17:1–5.
156. Rogers TA, Andrews GE, Jaeger L, Grabow WW. ACS synthetic biology. 2014; 4:162–166. [PubMed: 24932527]
157. Sato SI, Watanabe M, Katsuda Y, Murata A, Wang DO, Uesugi M. Angewandte Chemie. 2015; 127:1875–1878.
158. Yoo B, Kavishwar A, Ghosh SK, Barteneva N, Yigit MV, Moore A, Medarova Z. Chemistry & Biology. 2014; 21:199–204. [PubMed: 24440078]
159. Kang WJ, Cho YL, Chae JR, Lee JD, Ali BA, Al-Khedhairy AA, Lee CH, Kim S. Biomaterials. 2012; 33:6430–6437. [PubMed: 22698721]
160. Muramoto T, Cannon D, Gierlinski M, Corrigan A, Barton GJ, Chubb JR. Proceedings of the National Academy of Sciences of the United States of America. 2012; 109:7350–7355. [PubMed: 22529358]
161. Rino J, Martin RM, Carvalho T, Carmo-Fonseca M. Methods. 2014; 65:359–366. [PubMed: 23969316]
162. Vargas, Diana Y., Shah, K., Batish, M., Levandoski, M., Sinha, S., Marras, Salvatore AE., Schedl, P., Tyagi, S. Cell. 2011; 147:1054–1065. [PubMed: 22118462]
163. Buxbaum AR, Wu B, Singer RH. Science. 2014; 343:419–422. [PubMed: 24458642]
164. Wang Z, Zhang R, Wang Z, Wang HF, Wang Y, Zhao J, Wang F, Li W, Niu G, Kiesewetter DO, Chen X. ACS Nano. 2014; 8:12386–12396. [PubMed: 25494492]
165. Hayashi R, Wainwright SM, Liddell SJ, Pinchin SM, Horswell S, Ish-Horowicz D. G3-Genes Genomes Genetics. 2014; 4:749–760.
166. Pallavicini MG, George T, Deteresa PS, Amendola R, Gray JW. Journal of cellular physiology. 1994; 158:223–230. [PubMed: 8106559]
167. Zimyanin VL, Belaya K, Pecreaux J, Gilchrist MJ, Clark A, Davis I, St Johnston D. Cell. 2008; 134:843–853. [PubMed: 18775316]
168. van Gemert AMC, van der Laan AMA, Pilgram GSK, Fradkin LG, Noordermeer JN, Tanke HJ, Jost CR. Plos One. 2009; 4:e6663. [PubMed: 19684860]
169. Lee J, Kang HJ, Lee YS, Heo H, Gu HN, Cho S, Kim S. Chemical Communications. 2015; 51:7199–7202. [PubMed: 25811408]
170. Kam Y, Rubinstein A, Nissan A, Halle D, Yavin E. Molecular Pharmaceutics. 2012; 9:685–693. [PubMed: 22289057]
171. Viswanathan S, Williams ME, Bloss EB, Stasevich TJ, Speer CM, Nern A, Pfeiffer BD, Hooks BM, Li WP, English BP, Tian T, Henry GL, Macklin JJ, Patel R, Gerfen CR, Zhuang X, Wang Y, Rubin GM, Looger LL. Nat Meth. 2015; 12:568–576.
172. Park HY, Buxbaum AR, Singer RH. Methods in enzymology. 2010; 472:387–406. [PubMed: 20580973]
173. Annibale P, Gratton E. Transcription. 2014; 5:e28425. [PubMed: 25764219]
174. Saneyoshi H, Ito Y, Abe H. Journal of the American Chemical Society. 2013; 135:13632–13635. [PubMed: 24010717]

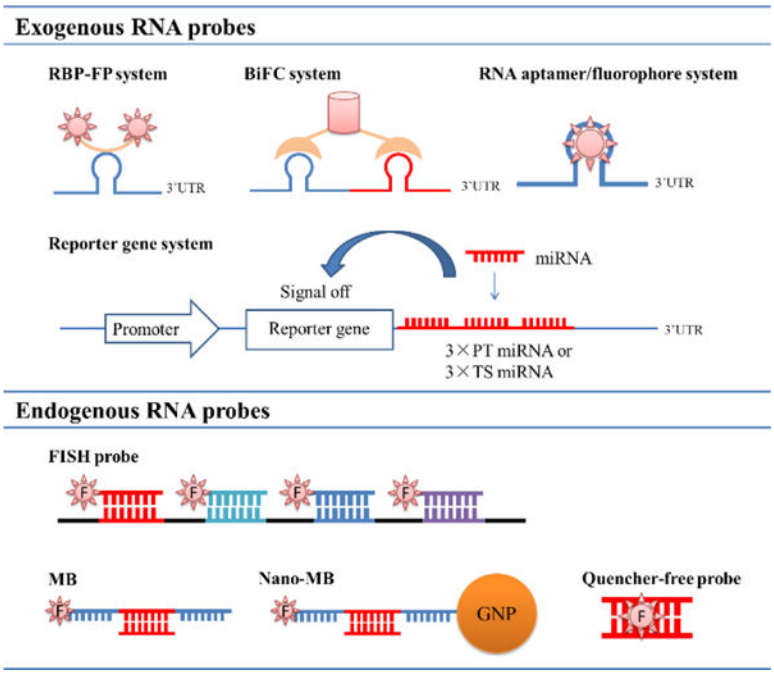

Fig. 1.

Graphical illustrations of various exogenous and endogenous RNA imaging probes binding to target RNAs, as discussed in this paper.

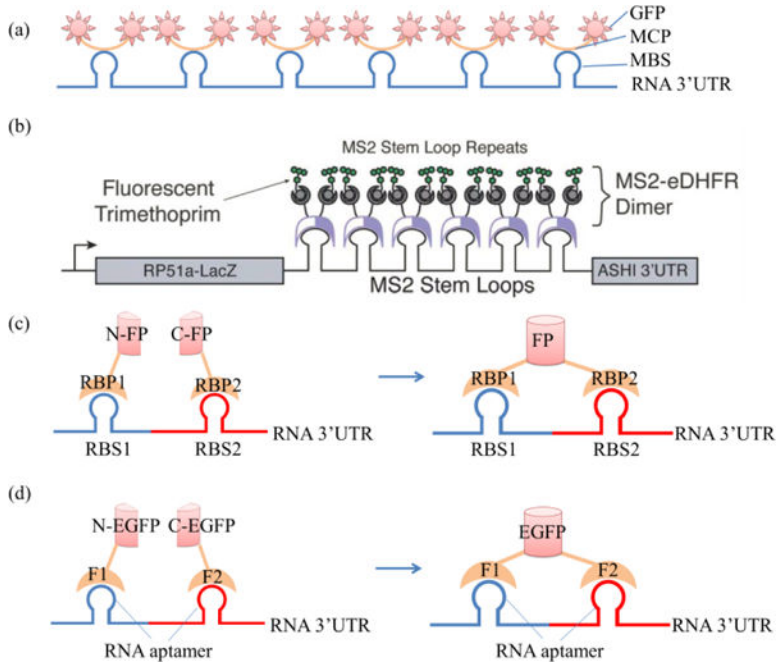

Fig. 2.

(a) Structure of the MS2-GFP based RBP-FP system: MCP, MS2 coat protein; MBS, MS2 binding sequence; UTR, untranslated region; (b) structure of MS2-eDHFR based RBP-FP system, adapted with permission from Carrocci and Hoskins[37]; (c) structure of the BiFC system: RBP, RNA binding protein; FP, fluorescent protein; RBS, BRP binding sequence; (d) structure of the aptamer-protein based BiFC system[38].

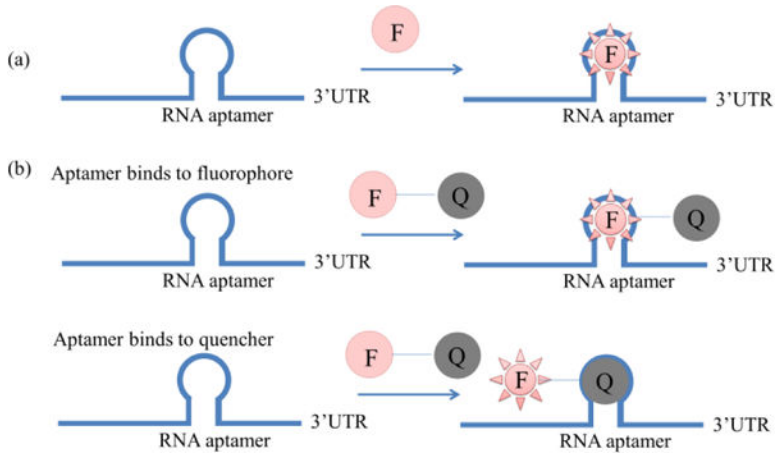

Fig. 3.

Different structures of RNA aptamer/fluorophore systems: (a) the initial RNA aptamer/fluorophore system,[47] where the RNA aptamer is pre-inserted into the 3′UTR of the target RNA and after the binding of fluorophore (F) to the RNA aptamer, the fluorescence of F will greatly increase; (b) two types of RNA aptamer/fluorophore system with quencher, one with aptamer binding to fluorophore[54] and one with aptamer binding to quencher[55].

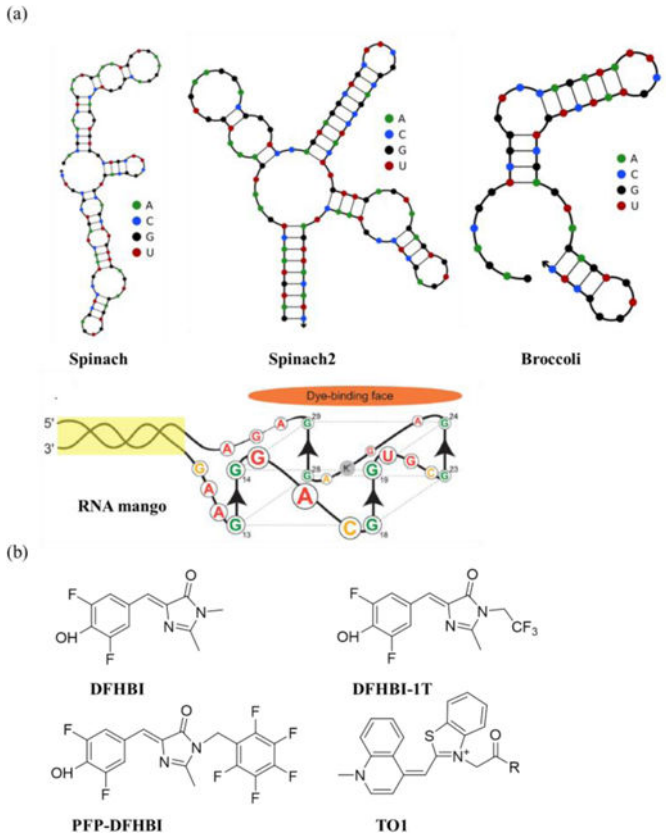

Fig. 4.

(a) Secondary structures of RNA aptamers in the RNA aptamer/fluorophore system: Spinach[47], Spinach2[49], Broccoli[52] and RNA mango[56]; structures of Spinach, Spinach2 and Broccoli were generated using the NUPACK online tool, and the structure of RNA mango was adapted with permission (ACS chemical biology 2014, 9 (10), 2412–2420, DOI: 10.1021/cb500499x),[56] Copyright (2014) American Chemical Society. (b) Chemical structures of fluorophores in the RNA aptamer/fluorophore systems: DFHBI, DFHBI-1T[57], PFP-DFHBI[58], TO1[56].

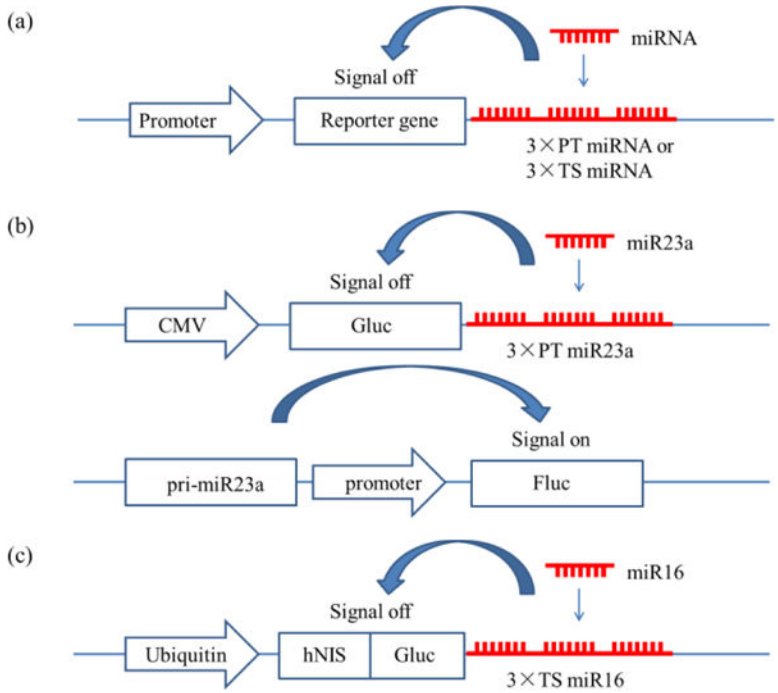

Fig. 5.

Structures of reporter gene systems: (a) the general structure of the reporter gene system, Promoter/Reporter gene/3×PT_miRNA or Promoter/Reporter gene/3×TS_miRNA[60]; (b) dual reporter gene systems with bioluminescence imaging,[73] CMV/Gluc/3×PT_miR23a and primiR23a/promoter/FLuc; (c) dual reporter gene systems with PET and biolumine-scence imaging,[74] ubiquitin/hNIS/Fluc/3×TS_miR16.

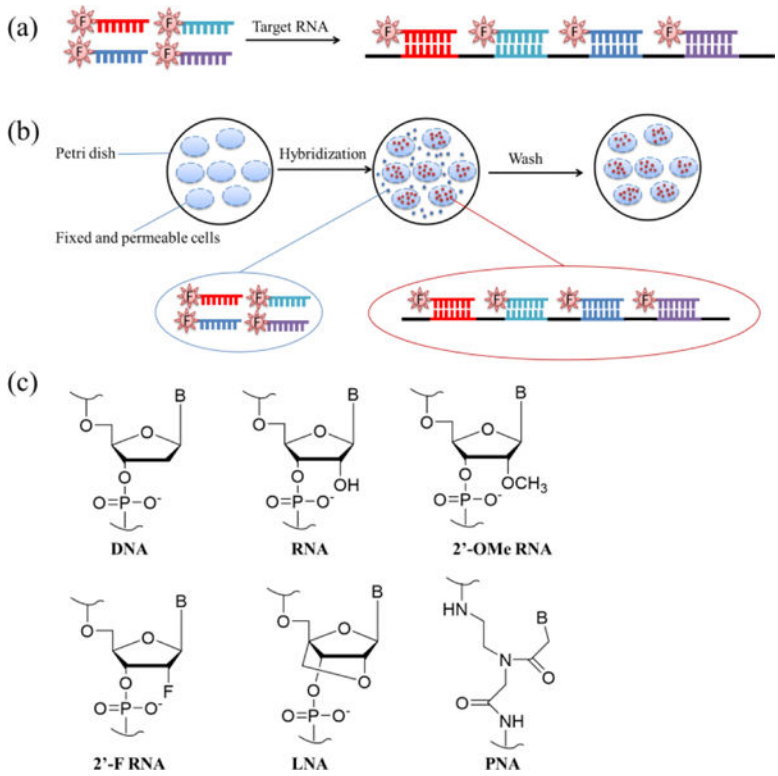

Fig. 6.

(a) Scheme of FISH probes, showing a group of ssDNAs labelled by the same fluorophore that can bind to different parts of target RNAs.[77, 79] (b) FISH procedures[33]: (i) fix cells and increase cell permeability; (ii) incubate FISH probes with cells and allow their hybridization with target RNAs; (iii) wash the cells to remove weakly bound FISH probes. (c) Chemical structures of chemically modified nucleic acids: 2′-OMe RNA, 2′-F RNA, LNA and PNA[81].

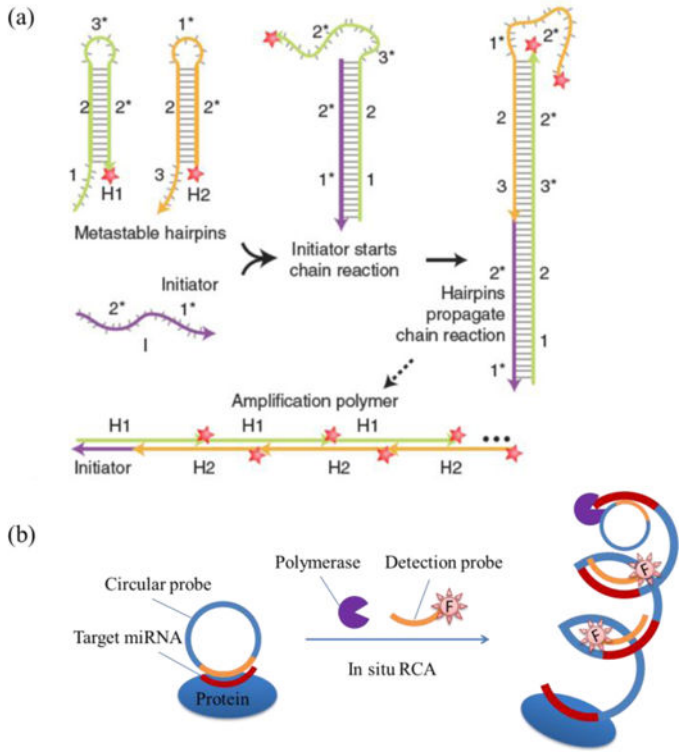

Fig. 7.

FISH based amplifications. (a) Hybridization chain reaction (HCR) amplification: (i) the initiator strand (containing the recognition strand and binding to target RNA before amplification begins) starts the chain reaction by forming a duplex with the H1 strand; (ii) initiator/H1 duplex propagates the reaction by forming a duplex with the H2 strand; (iii) the reaction is further continued by alternative binding of the H1 and H2 strand sequentially, and finally an amplification polymer with multiple fluorophores is formed. Adapted with permission from Macmillan Publishers Ltd., Nature Biotechnology[85], copyright (2010). (b) RCA amplification:[86] the circular probe first binds to target miRNA and then undergoes sequence elongation in the presence of polymerase and dNTP, followed by the binding of multiple detection probes, leading to signal amplification.

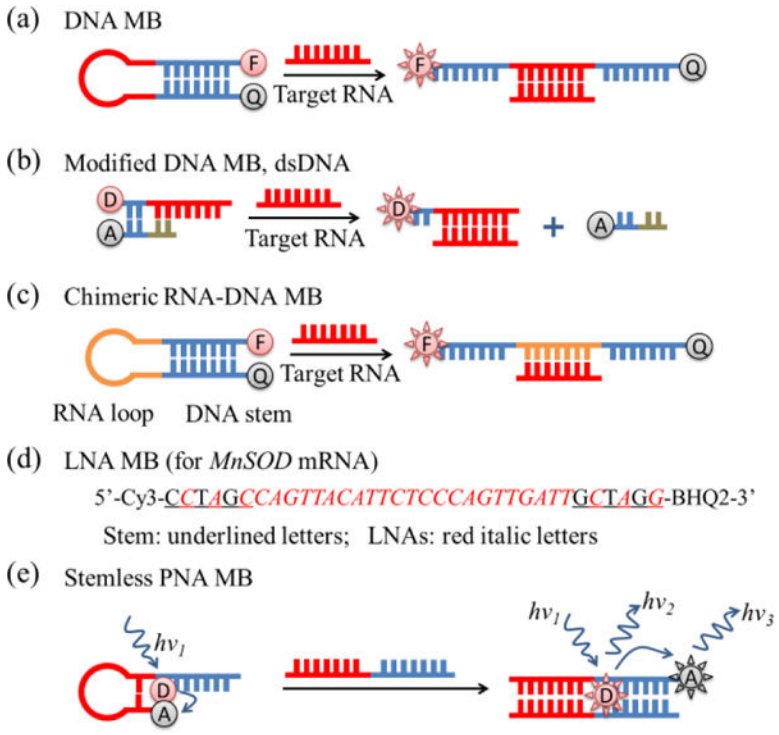

Fig. 8.

Different structures of MBs: (a) general DNA MBs with stem-loop structures; (b) modified MB: dsDNA with fluorophore donor and acceptor; (c) chimeric RNA-DNA molecular beacon with RNA loop and DNA stem[98]; (d) sequences of LNA MB with most LNAs remaining in the stem part and alternate LNAs in the loop part (red italic letters represent LNA bases, and underlined letters are bases for the MB stem)[99]; (e) stemless PNA MB[100].

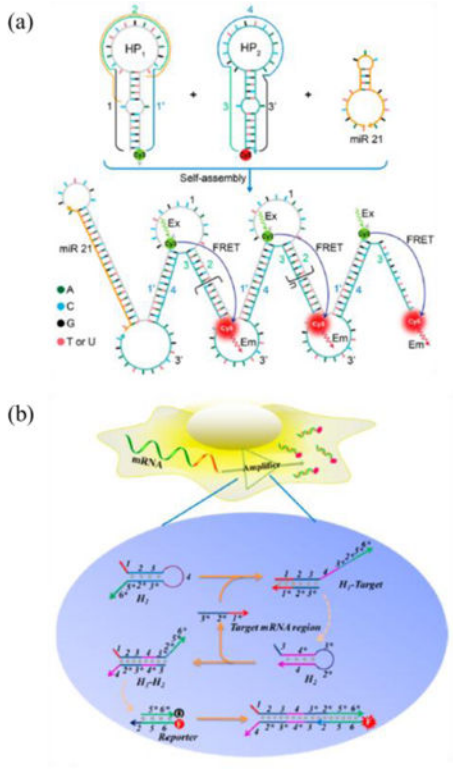

Fig. 9.

MBs with amplification methods: (a) HCR amplification, adapted with permission from (Journal of the American Chemical Society 2015, 137 (19), 6116–6119, DOI: 10.1021/jacs.5b01451)[101]. Copyright (2015) American Chemical Society; (b) CHR amplification, adapted from Wu *et al.*[103] with permission.

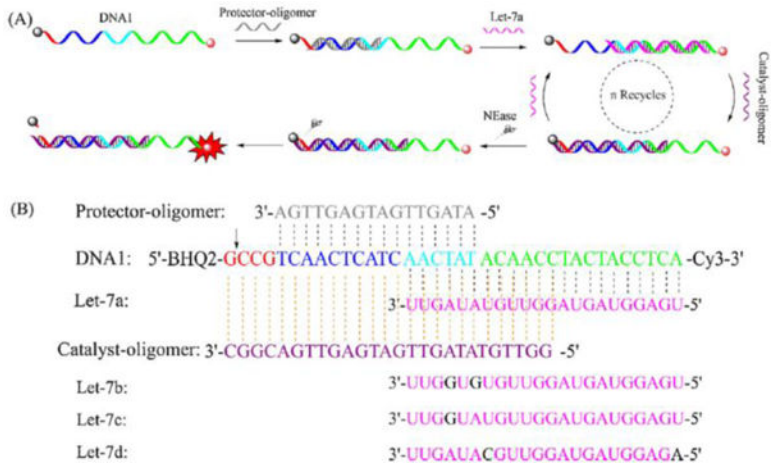

Fig. 10.

Enzyme enabled amplification[104]. Reprinted from Sensors and Actuators B: Chemical, 223, Zhang, K.; Wang, K.; Zhu, X.; Xie, M. A one-pot strategy for the sensitive detection of miRNA by catalyst–oligomer-mediated enzymatic amplification-based fluorescence biosensor, 586–590, Copyright (2016), with permission from Elsevier.

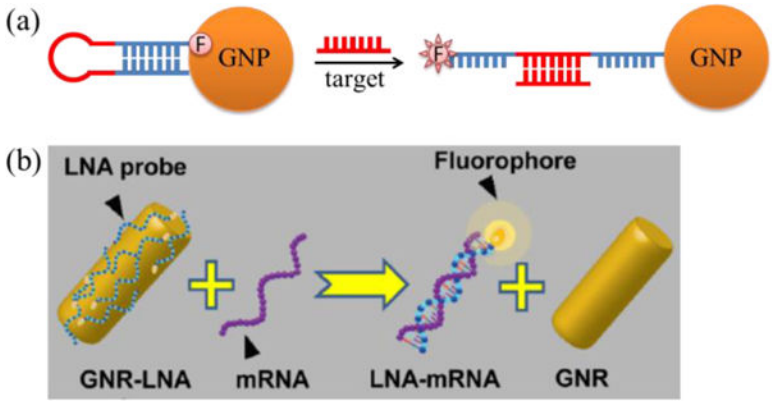

Fig. 11.

Structures of different Nano-MBs: (a) gold nanosphere based Nano-MB[120]; (b) gold nanorod based Nano-MB, adapted from Riahi *et al.* with permission[129].

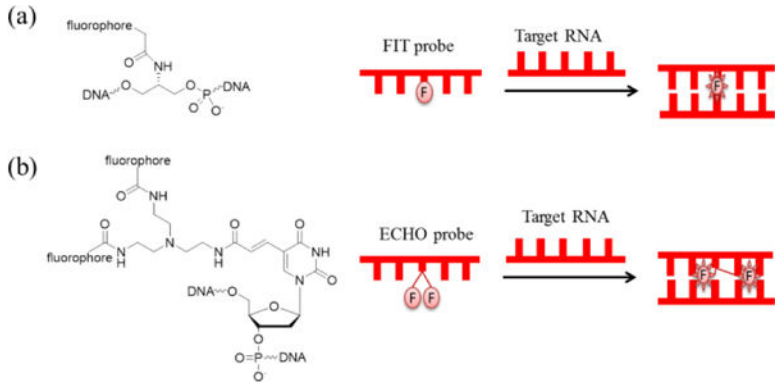

Fig. 12.

(a) Chemical structure of a typical FIT probe[146] and its imaging principle; (b) chemical structure of a typical ECHO probe[150] and its imaging principle.

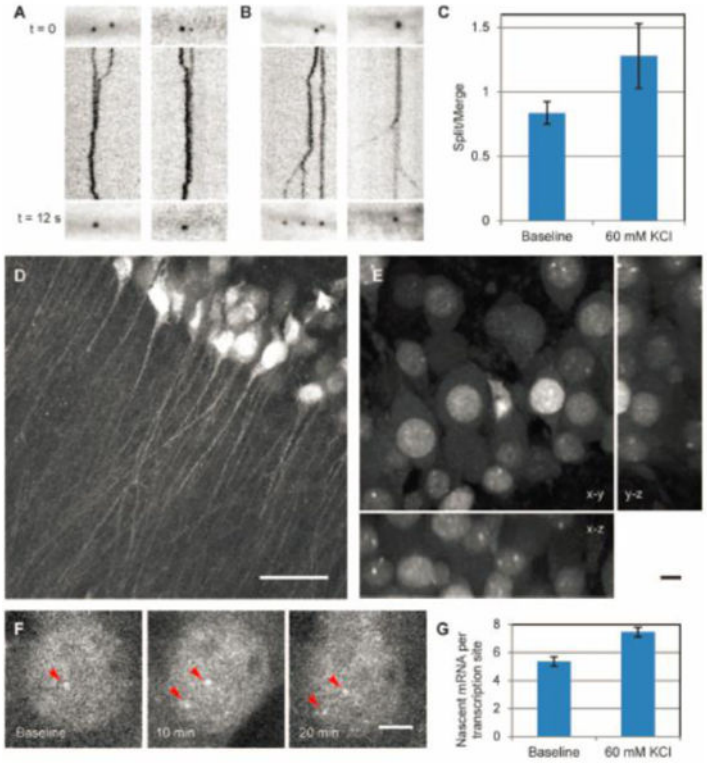

Fig. 13.

(A-B) The assembly (A) and disassembly (B) dynamics of the RBP-FP system labelled *β-actin* mRNP (RNA-protein complex) in neurons in 12 s with the lines showing the merging and splitting trajectories. (C) The ratio of split to merged events increased after KCl depolarization. (D) The CA1 region in the acute hippocampal slice. Scale bar, 50 μm. (E) The soma layer of CA1 neurons. Panels show maximum projections of x-y, y-z, and x-z planes. Scale bar, 10 μm. (F) Transcription of *β-actin* gene with KCl depolarization. Arrowheads denote *β-actin* transcription sites. Scale bar, 5 μm. (G) Nascent mRNA per transcription site increased after depolarization; [Science 2014, 343 (6169), 422–424, DOI: 10.1126/science.1239200][36]. Reprinted with permission from AAAS.

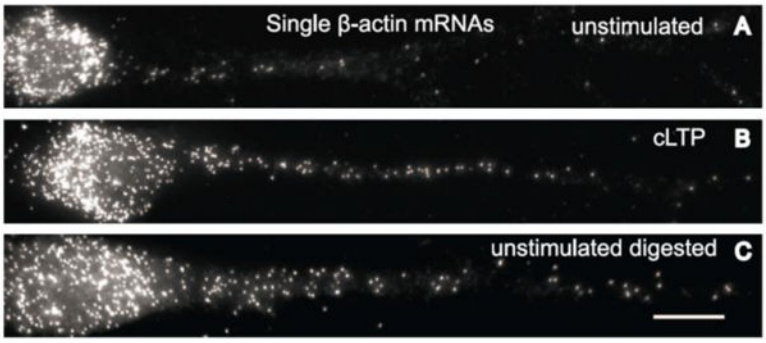

Fig. 14.

The distribution of single *β-actin* mRNA in dendrities without stimulation (A), with chemical long-term potentiation stimulation (B) and protease-digestion (C) detected by single-molecule FISH probes. Scale bar, 10 μm; [Science 2014, 343 (6169), 419–422, DOI: 10.1126/science.1242939][163]. Reprinted with permission from AAAS.

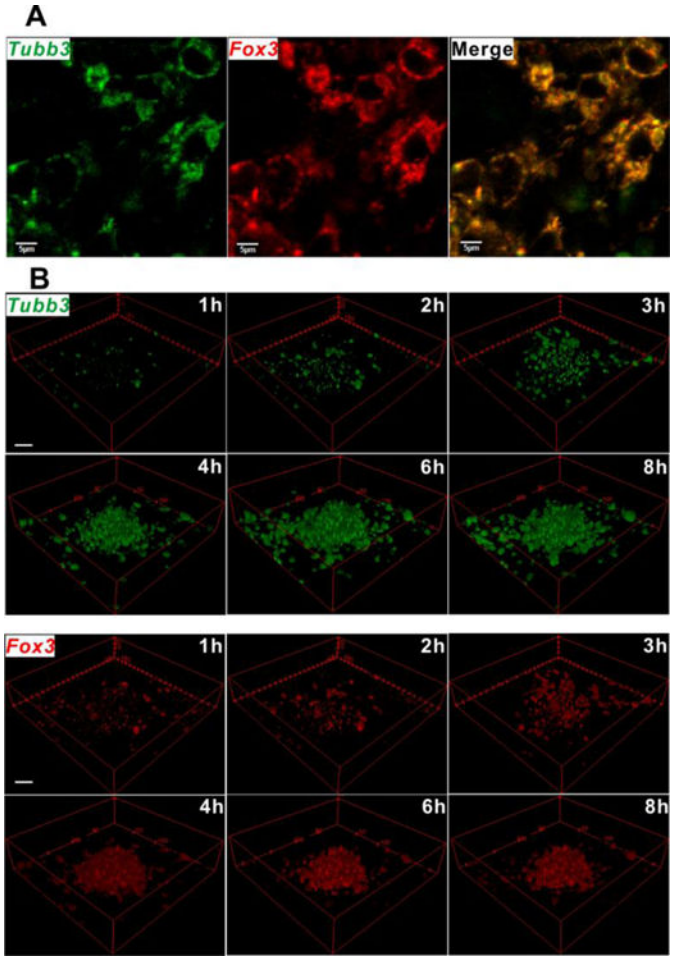

Fig. 15.

(A) Fluorescence imaging of *Tubb3* (green colour) and *Fox3* (red colour) mRNAs by fNCs (multifunctional nanocomplex, a GNP-Nano-MB) at day 8 in differentiated neural stem cells (NSCs) stimulated in advance by free retinoic acid. Scale = 5 μm. (B) Fluorescence recovery kinetics of fNCs in detecting *Tubb3* (green colour) and *Fox3* (red colour) mRNAs at day 8 in differentiated NSCs stimulated in advance by free RA. The images were reconstructed into 3D format for better illustration, without compromising the original. Scale = 20 μm. Adapted with permission from Wang *et al.*[164]

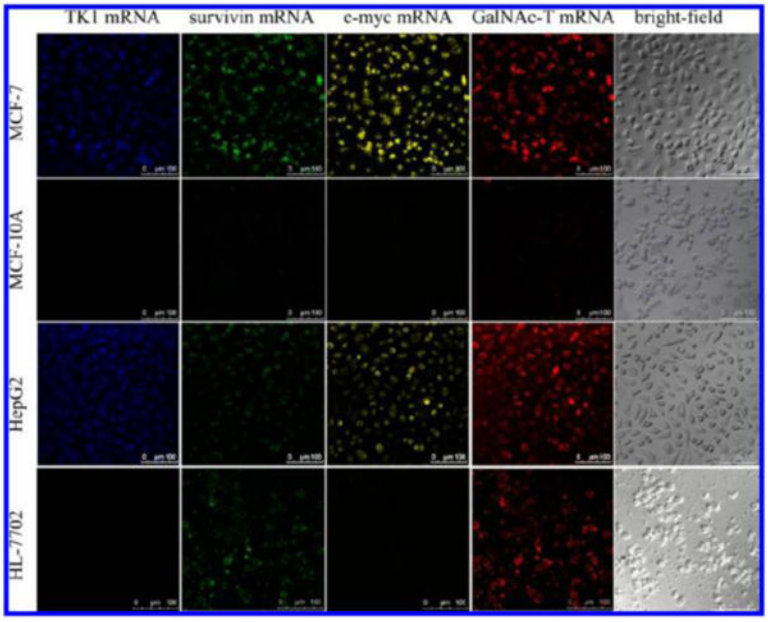

Fig. 16.

Intracellular imaging of *TK1* mRNA, *survivin* mRNA, *c-myc* mRNA, and *GalNAc-T* mRNA under CLSM. MCF-7, MCF-10A, HepG2, and HL-7702 cells were incubated with the GNP-Nano-MB (1 nM) for 3 h at 37 °C. The four mRNAs were recorded by Alexa Fluor 405 with 405-nm excitation, Alexa Fluor 488 with 488-nm excitation, Cy3 with 543-nm excitation, and Cy5 with 633-nm excitation. Scale bars = 100 μm. Reprinted with permission from Analytical chemistry 2013, 85 (21), 10581–10588, DOI: 10.1021/ac402700s)[132]. Copyright (2013) American Chemical Society.

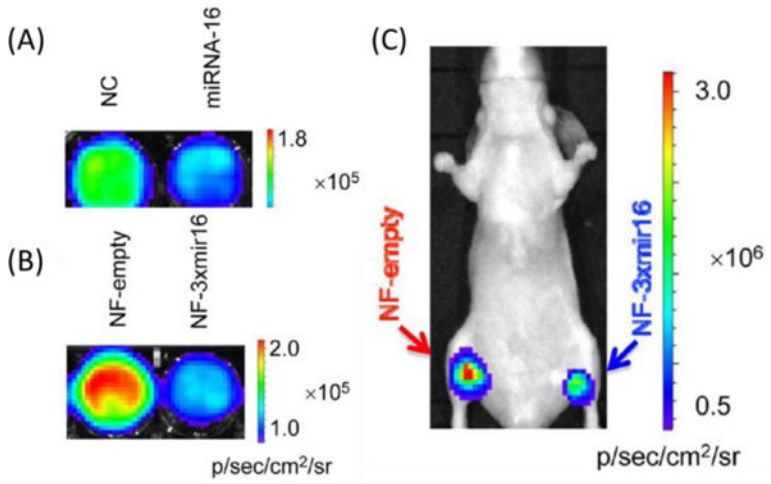

Fig. 17.

(A) *In vitro* bioluminescence imaging after transfecting miR16 or negative control (NC) RNA oligos (50 nM) into NF-3×mir16 cells. (B) *In vitro* bioluminescence imaging of NF(hNIS/Fluc fusion gene)-empty and NF-3×mir16 cells with equal numbers (1×10^6). (C) *In vivo* bioluminescence imaging of NF-empty and NF-3xmir xenografts with the same cell seeding density (1×10^7). Adapted from Wang *et al.*[74] with permission.

Table 1

Applications of RNA imaging probes in RNA process tracking

Target RNAs	Processes	Probe types
nascent mRNA	transcription	RBP-FP systems (MS2-GFP[160])
pre mRNA	splicesome assembly	RBP-FP system (MS2-mCherry[161])
***β-actin* mRNA**	transcription	FISH probe[77]
***β-actin* mRNA**	transcription, transport	RBP-FP system (Actb-MS2)[35, 36]
***β-actin* mRNA**	localization, transport	BiFC system (PUM-HD[1], PUM-HD mutants[43])
***β-actin* mRNA**	transport	Nano-MB (Sticky-Flare[123])
***β-actin* mRNA**	translation	FISH probe[163]
***gurken* mRNA**	localization, transport	RBP-FP system (MS2-mCherry[165])
***c-myc* mRNA**	transport	FISH probe[166]
***oskar* mRNA**	transport	RBP-FP system (MS2-GFP[167])
model mRNA	transport	RBP-FP system (MS2-GFP[168])
miR-124a	detection during neuronal differentiation	reporter gene system (CMV/Gluc/3×TS_miR124a[70])
miR-124a	detection during neuronal differentiation	MB(R9-QD-miR-124a beacon[111], miR-124a beacon[105])
miR-124a	detection during neurogenesis	MB (miR124a CMB[112])
miR-9	detection during neuronal differentiation	MB (Colour MB[106])
miR-23a	detection during neuronal differentiation	reporter gene system (CMV/Gluc/3×PT_miR23a[73])
miR-1	detection during myogenesis	reporter gene system (CMV/Gluc/3×PT_miR-1[159])
miR-1	detection during myogenic differentiation	Nano-MB (miR MRB[169])
miR-26a, miR-206	detection during myogenic differentiation	MB (miRNA-26a MB[107], miRNA-206 MB[107])
miR221	biogenesis in Papillary Thyroid Carcinoma	reporter gene system (CMV/Gluc/3×PT_miR221[68])

Table 2

Applications of RNA imaging probes in cancer diagnosis

Target RNAs	Cancer cell or tissue types	Probe types
***survivin* mRNA**	Hela, MCF-7 and SKBR-3	MB (HCR[113])
***survivin* mRNA**	HDF and MiaPaca-2	MB (peptide-MB[114])
***survivin* mRNA**	SKOV3[125], Hela[130]	Nano-MB (Nano-flare[125], Multiplexed Nanoflare[130])
***MnSOD* mRNA**	MDA-MB-231[103], MCF-7[115]	MB(HDCA[103], CP/MB probe[115])
***c-raf-1* mRNA**	A549	Nano-MB (DNA Micelle Flare[119])
***TK1* mRNA**	HepG2, MCF-7	Nano-MB (FRET nanoflare[124])
***STAT5B* mRNA**	MCF-7	Nano-MB (GNP beacon[126])
***K-ras* mRNA**	Panc-1, sw-480	MB (PNA-MB[170])
***TK1*/*GalNac* mRNA**	HepG2, MCF-7	Nano-MB (fluorescence Nanoprobe[121])
***TK1*/*survivin* mRNA**	HepG2, MCF-7	Nano-MB (FRET Nanoprobe[133])
***c-myc*/*TK1*/*GalNac-T* mRNA**	HepG2, MCF-7	Nano-MB (Multicolour Nanoprobe[131])
***c-myc*/*TK1*/*GalNac-T*/*survivin* mRNA**	HepG2, MCF-7	Nano-MB (Four-colour Nanoprobe[132])
miR21	A549	reporter gene system (CMV/Fluc/3×TS_miR21[67])
miR16	SGC7901, SGC7901/VCR	reporter gene system (CMV/hNIS/Fluc/3×TS_miR16[74])
miR21	Hela	MB (HCR[101])
miR21	MCF-7, HepG2	MB (ONAA-PCMSN[110])
miR21	pancreatic ductal adenocarcinoma	FISH probe (LNA-FISH[5])
miR15a	MDA-MB-231, Hela	FISH probe (LNA-ELF-FISH[11])
miR155	MCF-7	FISH probe (LNA-ELF-FISH[11])
***let-7a* miRNA**	A549	MB (TIRCA[87], CEMA[104])
miR-34a	MCF-7	MB (CF probe[116])
miR-122	Huh-7, HepG2, Hela, MDA-MB-231	Nano-MB (AuNP hairpin[127])
miR-10b	MDA-MB-231-luc-D3H2LN	ssRNA[158]